

1 **Mitochondrial respiratory states and rates:**  
2 **Building blocks of mitochondrial physiology Part 1**  
3

4 **COST Action CA15203 MitoEAGLE preprint** Version: 2018-04-01(37)

5 Corresponding author: Gnaiger E

6 Co-authors:

7 Aasander Frostner E, Abumrad NA, Acuna-Castroviejo D, Ahn B, Ali SS, Alves MG, Amati  
8 F, Aral C, Arandarčikaitė O, Bailey DM, Bajpeyi S, Bakker BM, Bastos Sant'Anna Silva AC,  
9 Battino M, Bazil J, Beard DA, Bednarczyk P, Ben-Shachar D, Bergdahl A, Bernardi P,  
10 Bishop D, Blier PU, Boetker HE, Boros M, Borsheim E, Borutaitė V, Bouillaud F, Boutbir J,  
11 Breton S, Brown DA, Brown GC, Brown RA, Brozinick JT, Buettner GR, Burtscher J,  
12 Calabria E, Calbet JA, Calzia E, Cannon DT, Canto AC, Cardoso LHD, Carvalho E, Casado  
13 Pinna M, Cassina AM, Castro L, Cavalcanti-de-Albuquerque JP, Cervinkova Z, Chang SC,  
14 Chaurasia B, Chen Q, Chicco AJ, Chinopoulos C, Chowdhury SK, Clementi E, Coen PM,  
15 Coker RH, Collin A, Crisóstomo L, Darveau CA, Das AM, Dash RK, Davis MS, De Palma C,  
16 Dembinska-Kiec A, Dias TR, Distefano G, Doerrier C, Drahota Z, Dubouchaud H, Duchon  
17 MR, Dumas JF, Durham WJ, Dymkowska D, Dyrstad SE, Dzialowski EM, Ehinger J, Elmer  
18 E, Endlicher R, Engin AB, Fell DA, Ferko M, Ferreira JCB, Ferreira R, Fessel JP, Filipovska  
19 A, Fisar Z, Fischer M, Fisher G, Fisher JJ, Fornaro M, Galkin A, Gan Z, Garcia-Roves PM,  
20 Garcia-Souza LF, Garlid KD, Garrabou G, Garten A, Gastaldelli A, Genova ML, Giovarelli  
21 M, Gonzalez-Armenta JL, Gonzalo H, Goodpaster BH, Gorr TA, Gourlay CW, Granata C,  
22 Grefte S, Haas CB, Haavik J, Haendeler J, Hamann A, Han J, Hancock CR, Hand SC,  
23 Hargreaves IP, Harrison DK, Heales SJR, Hellgren KT, Hepple RT, Hernansanz-Agustin P,  
24 Hickey AJ, Hoel F, Holland OJ, Holloway GP, Hoppel CL, Houstek J, Hunger M, Iglesias-  
25 Gonzalez J, Irving BA, Iyer S, Jackson CB, Jadiya P, Jang DH, Jang YC, Jansen-Dürr P,  
26 Jespersen NR, Jha RK, Jurk D, Kaambre T, Kaczor JJ, Kainulainen H, Kandel SM, Kane DA,  
27 Kappler L, Karabatsiakos A, Karkucinska-Wieckowska A, Keijer J, Keppner G, Khamoui AV,  
28 Klingenspor M, Komlodi T, Koopman WJH, Kopitar-Jerala N, Kowaltowski AJ, Krajcova A,  
29 Krako Jakovljevic N, Kristal BS, Kuang J, Kucera O, Kwak HB, Kwast K, Labieniec-Watala  
30 M, Lai N, Land JM, Lane N, Laner V, Lanza IR, Larsen TS, Lavery GG, Lee HK,  
31 Leeuwenburgh C, Lemieux H, Lerfall J, Li PA, Liu J, Lucchinetti E, Macedo MP,  
32 MacMillan-Crow LA, Makrecka-Kuka M, Malik A, Markova M, Martin DS, Mazat JP,  
33 McKenna HT, Menze MA, Meszaros AT, Methner A, Michalak S, Moellering DR, Moiso N,  
34 Molina AJA, Montaigne D, Moreau K, Moore AL, Moreira BP, Mracek T, Muntane J,  
35 Muntean DM, Murray AJ, Nair KS, Nemeč M, Neuffer PD, Neuzil J, Newsom S, Nozickova  
36 K, O'Gorman D, Oliveira MF, Oliveira MT, Oliveira PF, Oliveira PJ, Orynbayeva Z,  
37 Osiewacz HD, Pak YK, Pallotta ML, Palmeira CM, Parajuli N, Passos JF, Patel HH, Pecina  
38 P, Pelna D, Pereira da Silva Grilo da Silva F, Pesta D, Petit PX, Pettersen IKN, Pichaud N,  
39 Piel S, Pietka TA, Pino MF, Pirkmajer S, Porter C, Porter RK, Pranger F, Prochownik EV,  
40 Pulinilkunnil T, Puskarich MA, Puurand M, Quijano C, Radenkovic F, Radi R, Ramzan R,  
41 Rattan S, Reboredo P, Renner-Sattler K, Robinson MM, Roden M, Rohlena J, Rolo AP,  
42 Ropelle ER, Røslund GV, Rossiter HB, Rybacka-Mossakowska J, Saada A, Safaei Z, Salin K,  
43 Salvadego D, Sandi C, Sanz A, Sazanov LA, Scatena R, Schartner M, Scheibye-Knudsen M,  
44 Schilling JM, Schlattner U, Schönfeld P, Schwarzer C, Scott GR, Shabalina IG, Sharma P,  
45 Sharma V, Shevchuk I, Siewiera K, Silber AM, Silva AM, Sims CA, Singer D, Skolik R,  
46 Smenes BT, Smith J, Soares FAA, Sobotka O, Sokolova I, Sonkar VK, Sparagna GC, Sparks  
47 LM, Spinazzi M, Stankova P, Stary C, Stier A, Stocker R, Sumbalova Z, Suravajhala P,  
48 Swerdlow RH, Swiniuch D, Szabo I, Szewczyk A, Tanaka M, Tandler B, Tarnopolsky MA,  
49 Tavernarakis N, Tepp K, Thyfault JP, Tomar D, Towheed A, Tretter L, Trifunovic A,  
50 Trivigno C, Tronstad KJ, Trougakos IP, Tyrrell DJ, Urban T, Valentine JM, Velika B,  
51 Vendelin M, Vercesi AE, Victor VM, Vieyra A Villena JA, Vitorino RMP, Vogt S, Volani C,

Votion DM, Vujacic-Mirski K, Wagner BA, Ward ML, Warnsmann V, Wasserman DH,  
 Watala C, Wei YH, Wieckowski MR, Williams C, Wohlgemuth SE, Wohlwend M, Wolff J,  
 Wüst RCI, Yokota T, Zablocki K, Zaugg K, Zaugg M, Zhang Y, Zhang YZ, Zischka H,  
 Zorzano A

### Updates and discussion:

[http://www.mitoeagle.org/index.php/MitoEAGLE\\_preprint\\_2018-02-08](http://www.mitoeagle.org/index.php/MitoEAGLE_preprint_2018-02-08)

Correspondence: Gnaiger E

Chair COST Action CA15203 MitoEAGLE – <http://www.mitoeagle.org>

Department of Visceral, Transplant and Thoracic Surgery, D. Swarovski Research  
 Laboratory, Medical University of Innsbruck, Innrain 66/4, A-6020 Innsbruck, Austria

Email: [mitoeagle@i-med.ac.at](mailto:mitoeagle@i-med.ac.at); Tel: +43 512 566796, Fax: +43 512 566796 20

### Abstract - Executive summary

**1. Introduction** – Box 1: In brief: Mitochondria and Bioblasts

**2. Oxidative phosphorylation and coupling states in mitochondrial preparations**

Mitochondrial preparations

2.1. *Respiratory control and coupling*

The steady-state

Specification of biochemical dose

Phosphorylation,  $P_{\gg}$ , and  $P_{\gg}/O_2$  ratio

Control and regulation

Respiratory control and response

Respiratory coupling control and ET-pathway control

Coupling

Uncoupling

2.2. *Coupling states and respiratory rates*

Respiratory capacities in coupling control states

LEAK, OXPHOS, ET, ROX

Quantitative relations

2.3. *Classical terminology for isolated mitochondria*

States 1–5

**3. Normalization: flows and fluxes**

3.1. *Normalization: system or sample*

Flow per system,  $I$

Extensive quantities

Size-specific quantities – Box 2: Metabolic flows and fluxes: vectorial and scalar

3.2. *Normalization for system-size: flux per chamber volume*

System-specific flux,  $J_{V,O_2}$

3.3. *Normalization: per sample*

Sample concentration,  $C_{mX}$

Mass-specific flux,  $J_{O_2/mX}$

Number concentration,  $C_{NX}$

Flow per object,  $I_{O_2/X}$

3.4. *Normalization for mitochondrial content*

Mitochondrial concentration,  $C_{mtE}$ , and mitochondrial markers

Mitochondria-specific flux,  $J_{O_2/mtE}$

3.5. *Evaluation of mitochondrial markers*

3.6. *Conversion: units*

**4. Conclusions** – Box 3: Recommendations for studies with mitochondrial preparations

**References**

104 **Abstract** As the knowledge base and importance of mitochondrial physiology to human health  
 105 expands, the necessity for harmonizing the terminology concerning mitochondrial respiratory  
 106 states and rates has become increasingly apparent. The chemiosmotic theory establishes the  
 107 mechanism of energy transformation and coupling in oxidative phosphorylation. The unifying  
 108 concept of the protonmotive force provides the framework for developing a consistent  
 109 theoretical foundation of mitochondrial physiology and bioenergetics. We follow IUPAC  
 110 guidelines on terminology in physical chemistry, extended by considerations on open systems  
 111 and irreversible thermodynamics. The concept-driven constructive terminology incorporates  
 112 the meaning of each quantity and aligns concepts and symbols to the nomenclature of classical  
 113 bioenergetics. In the frame of COST Action MitoEAGLE open to global bottom-up input, we  
 114 endeavour to provide a balanced view on mitochondrial respiratory control and a critical  
 115 discussion on reporting data of mitochondrial respiration in terms of metabolic flows and fluxes.  
 116 Uniform standards for evaluation of respiratory states and rates will ultimately support the  
 117 development of databases of mitochondrial respiratory function in species, tissues, and cells.  
 118 Clarity of concept and consistency of nomenclature facilitate effective transdisciplinary  
 119 communication, education, and ultimately further discovery.

120

121 *Keywords:* Mitochondrial respiratory control, coupling control, mitochondrial  
 122 preparations, protonmotive force, uncoupling, oxidative phosphorylation, OXPHOS,  
 123 efficiency, electron transfer, ET; proton leak, LEAK, residual oxygen consumption, ROX, State  
 124 2, State 3, State 4, normalization, flow, flux, O<sub>2</sub>

125

126

---

## 126 **Executive summary**

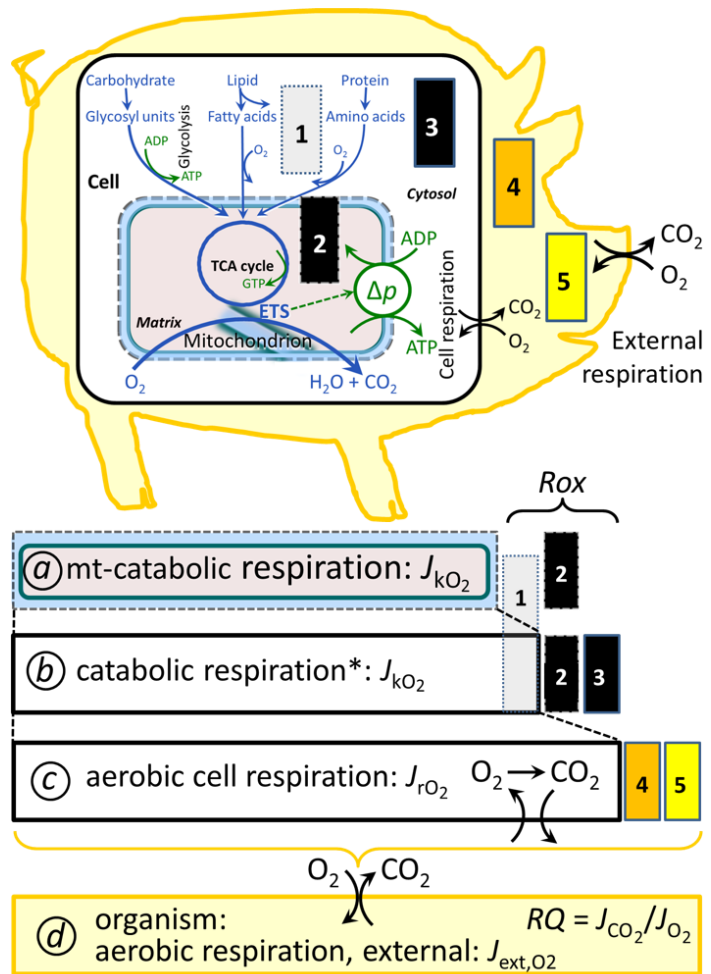
127

128 1. In view of the broad implications for health care, mitochondrial researchers face an  
 129 increasing responsibility to disseminate their fundamental knowledge and novel  
 130 discoveries to a wide range of stakeholders and scientists beyond the group of  
 131 specialists. This requires implementation of a commonly accepted terminology  
 132 within the discipline and standardization in the translational context. Authors,  
 133 reviewers, journal editors, and lecturers are challenged to collaborate with the aim  
 134 to harmonize the nomenclature in the growing field of mitochondrial physiology  
 135 and bioenergetics, from evolutionary biology and comparative physiology to  
 136 mitochondrial medicine.

137 2. Aerobic respiration depends on the coupling of phosphorylation (ADP → ATP) to O<sub>2</sub>  
 138 flux in catabolic reactions. Coupling in oxidative phosphorylation is mediated by  
 139 translocation of protons across the inner mitochondrial membrane through proton  
 140 pumps generating or utilizing the protonmotive force, that is measured between the  
 141 mitochondrial matrix and intermembrane compartment or outer mitochondrial  
 142 space. Compartmental coupling distinguishes vectorial oxidative phosphorylation  
 143 from glycolytic fermentation as the counterpart of cellular core energy metabolism  
 144 (**Figure 1**).

145 3. To exclude fermentation and other cytosolic interactions from exerting an effect on the  
 146 analysis of mitochondrial metabolism, the barrier function of the plasma membrane  
 147 must be disrupted. Selective removal or permeabilization of the plasma membrane  
 148 yields mitochondrial preparations—including isolated mitochondria, tissue and  
 149 cellular preparations—with structural and functional integrity. Then extra-  
 150 mitochondrial concentrations of fuel substrates, ADP, ATP, inorganic phosphate,  
 151 and cations including H<sup>+</sup> can be controlled to determine mitochondrial function  
 152 under a set of conditions defined as coupling control states. A concept-driven  
 153 terminology of bioenergetics explicitly incorporates in its terms and symbols  
 154 information on the nature of respiratory states that makes the technical terms readily  
 155 recognized and more easy to understand.

156 **Figure 1. Mitochondrial respiration**  
 157 **is the oxidation of fuel substrates**  
 158 **(electron donors) and reduction of**  
 159 **O<sub>2</sub> catalysed by the electron**  
 160 **transfer system, ETS:** (a)  
 161 **mitochondrial catabolic**  
 162 **respiration;** (b) **mitochondrial and**  
 163 **non-mitochondrial catabolic O<sub>2</sub>**  
 164 **consumption;** O<sub>2</sub> **balance of (c) total**  
 165 **cellular O<sub>2</sub> consumption and (d)**  
 166 **external respiration**



167 All chemical reactions,  $r$ , that  
 168 consume O<sub>2</sub> in the cells of an  
 169 organism, contribute to cell  
 170 respiration,  $J_{rO_2}$ . ❶ Non-mitochondrial  
 171 O<sub>2</sub> consumption by catabolic  
 172 reactions, particularly peroxisomal  
 173 oxidases; ❷ mitochondrial residual  
 174 oxygen consumption,  $Rox$ , after  
 175 blocking the ETS; ❸ non-  
 176 mitochondrial  $Rox$ ; ❹ extracellular O<sub>2</sub>  
 177 consumption; ❺ aerobic microbial  
 178 respiration. Bars are not at a  
 179 quantitative scale.

180 **a Mitochondrial catabolic**  
 181 **respiration,  $J_{kO_2}$ , is the O<sub>2</sub>**  
 182 **consumption by the mitochondrial**  
 183 **ETS maintaining the protonmotive force,  $\Delta p$ .  $J_{kO_2}$  excludes  $Rox$ .**

184 **b Catabolic respiration** is the O<sub>2</sub> consumption associated with catabolic pathways in the cell,  
 185 including peroxisomal oxidation reactions (❶) in addition to mitochondrial catabolism (\*  
 186 The reactions  $k$  have to be defined specifically for  $a$  and  $b$ .)

187 **c Aerobic cell respiration,  $J_{rO_2}$ , takes into account internal O<sub>2</sub>-consuming reactions,  $r$ ,**  
 188 including catabolic respiration and  $Rox$ . Internal respiration of an organism includes  
 189 extracellular O<sub>2</sub> consumption (❹) and aerobic respiration by the microbiome (❺).  
 190 Respiration is distinguished from fermentation by: (1) External electron acceptors for the  
 191 maintenance of redox balance, whereas fermentation is characterized by an internal electron  
 192 acceptor produced in intermediary metabolism. In aerobic cell respiration, redox balance is  
 193 maintained by O<sub>2</sub> as the electron acceptor. (2) Compartmental coupling in vectorial oxidative  
 194 phosphorylation, in contrast to exclusively scalar substrate-level phosphorylation in  
 195 fermentation.

196 **d External respiration** balances internal respiration at steady-state. O<sub>2</sub> is transported from the  
 197 environment across the respiratory cascade (circulation between tissues and diffusion across  
 198 cell membranes) to the intracellular compartment, while bicarbonate and CO<sub>2</sub> are transported  
 199 in reverse to the extracellular milieu and the organismic environment. Hemoglobin provides  
 200 the molecular paradigm for the combination of O<sub>2</sub> and CO<sub>2</sub> exchange, as do lungs and gills  
 201 on the morphological level. The respiratory quotient,  $RQ$ , is the molar CO<sub>2</sub>/O<sub>2</sub> exchange  
 202 ratio; when combined with the respiratory nitrogen quotient, N/O<sub>2</sub> (mol N given off per mol  
 203 O<sub>2</sub> consumed), the  $RQ$  reflects the proportion of carbohydrate, lipid and protein utilized in  
 204 cell respiration during aerobically balanced steady-states.

205

- 206 4. Mitochondrial coupling states are defined according to the control of respiratory oxygen  
 207 flux by the protonmotive force. Capacities of oxidative phosphorylation and  
 208 electron transfer are measured at kinetically saturating concentrations of fuel  
 209 substrates, ADP and inorganic phosphate, or at optimal uncoupler concentrations,  
 210 respectively, in the absence of Complex IV inhibitors such as NO, CO, or H<sub>2</sub>S.  
 211 Respiratory capacity is a measure of the upper bound of the rate of respiration,  
 212 depends on the substrate type undergoing oxidation, and provides reference values  
 213 for the diagnosis of health and disease, and for evaluation of the effects of  
 214 Evolutionary background, Age, Gender and sex, Lifestyle and Environment  
 215 (EAGLE).
- 216 5. Incomplete tightness of coupling, *i.e.*, some degree of uncoupling relative to the  
 217 substrate-dependent coupling stoichiometry, is a characteristic of energy-  
 218 transformations across membranes. Uncoupling is caused by a variety of  
 219 physiological, pathological, toxicological, pharmacological and environmental  
 220 conditions that exert an influence not only on the proton leak and cation cycling,  
 221 but also on proton slip within the proton pumps and the structural integrity of the  
 222 mitochondria. A more loosely coupled state is induced by stimulation of  
 223 mitochondrial superoxide formation and the bypass of proton pumps. In addition,  
 224 uncoupling by application of protonophores represents an experimental  
 225 intervention for the transition from a well-coupled to the noncoupled state of  
 226 mitochondrial respiration.
- 227 6. Respiratory oxygen consumption rates have to be carefully normalized to enable meta-  
 228 analytic studies beyond the specific question of a particular experiment. Therefore,  
 229 all raw data should be published in a supplemental table or open access data  
 230 repository. Normalization of rates for the volume of the experimental chamber (the  
 231 measuring system) is distinguished from normalization for: (1) the volume or mass  
 232 of the experimental sample; (2) the number of objects (cells, organisms); and (3)  
 233 the concentration of mitochondrial markers in the chamber.
- 234 7. The consistent use of terms and symbols will facilitate transdisciplinary communication  
 235 and support further developments of a database on bioenergetics and mitochondrial  
 236 physiology. The present considerations are focused on studies with mitochondrial  
 237 preparations. These will be extended in a series of reports on pathway control of  
 238 mitochondrial respiration, the protonmotive force, respiratory states in intact cells,  
 239 and harmonization of experimental procedures.  
 240

---

### 241 **Box 1: In brief – Mitochondria and Bioblasts**

242  
 243 *‘For the physiologist, mitochondria afforded the first opportunity for an*  
 244 *experimental approach to structure-function relationships, in particular those*  
 245 *involved in active transport, vectorial metabolism, and metabolic control*  
 246 *mechanisms on a subcellular level’ (Ernster and Schatz 1981).*  
 247

248 **Mitochondria** are the oxygen-consuming electrochemical generators evolved from  
 249 endosymbiotic bacteria (Margulis 1970; Lane 2005). They were described by Richard Altmann  
 250 (1894) as ‘bioblasts’, which include not only the mitochondria as presently defined, but also  
 251 symbiotic and free-living bacteria. The word ‘mitochondria’ (Greek mitos: thread; chondros:  
 252 granule) was introduced by Carl Benda (1898).

253 Mitochondria form dynamic networks within eukaryotic cells and are morphologically  
 254 enclosed by a double membrane. The mitochondrial inner membrane (mtIM) shows dynamic  
 255 tubular to disk-shaped cristae that separate the mitochondrial matrix, *i.e.*, the negatively charged  
 256 internal mitochondrial compartment, from the intermembrane space; the latter being enclosed  
 257 by the mitochondrial outer membrane (mtOM) and positively charged with respect to the

258 matrix. The mtIM contains the non-bilayer phospholipid cardiolipin, which is not present in  
259 any other eukaryotic cellular membrane. Cardiolipin stabilizes and promotes the formation of  
260 respiratory supercomplexes (SC I<sub>n</sub>III<sub>n</sub>IV<sub>n</sub>), which are supramolecular assemblies based upon  
261 specific, though dynamic interactions between individual respiratory complexes (Greggio *et al.*  
262 2017; Lenaz *et al.* 2017). Membrane fluidity exerts an influence on functional properties of  
263 proteins incorporated in the membranes (Waczulikova *et al.* 2007). In addition to mitochondrial  
264 movement along microtubules, mitochondrial morphology can change in response to energy  
265 requirements of the cell via processes known as fusion and fission, through which mitochondria  
266 communicate within a network (Chan 2006). Intracellular stress factors may cause shrinking or  
267 swelling of the mitochondrial matrix, that can ultimately result in permeability transition.

268 Mitochondria are the structural and functional elements of cell respiration. Mitochondrial  
269 respiration is the reduction of molecular oxygen by electron transfer coupled to electrochemical  
270 proton translocation across the mtIM. In the process of oxidative phosphorylation (OXPHOS),  
271 the catabolic reaction of oxygen consumption is electrochemically coupled to the  
272 transformation of energy in the form of adenosine triphosphate (ATP; Mitchell 1961, 2011).  
273 Mitochondria are the powerhouses of the cell which contain the machinery of the OXPHOS-  
274 pathways, including transmembrane respiratory complexes (proton pumps with FMN, Fe-S and  
275 cytochrome *b*, *c*, *aa*<sub>3</sub> redox systems); alternative dehydrogenases and oxidases; the coenzyme  
276 ubiquinone (Q); F-ATPase or ATP synthase; the enzymes of the tricarboxylic acid cycle, fatty  
277 acid and amino acid oxidation; transporters of ions, metabolites and co-factors; iron/sulphur  
278 cluster synthesis; and mitochondrial kinases related to energy transfer pathways. The  
279 mitochondrial proteome comprises over 1,200 proteins (Calvo *et al.* 2015; 2017), mostly  
280 encoded by nuclear DNA (nDNA), with a variety of functions, many of which are relatively  
281 well known (*e.g.*, proteins regulating mitochondrial biogenesis or apoptosis), while others are  
282 still under investigation, or need to be identified (*e.g.*, alanine transporter). Only lately it is  
283 possible to use the mammalian mitochondrial proteome to discover and characterize the genetic  
284 basis of mitochondrial diseases (Williams *et al.* 2016; Palmfeldt and Bross 2017).

285 There is a constant crosstalk between mitochondria and the other cellular components.  
286 The crosstalk between mitochondria and endoplasmic reticulum is involved in the regulation of  
287 calcium homeostasis, cell division, autophagy, differentiation, and anti-viral signaling (Murley  
288 and Nunnari 2016). Mitochondria contribute to the formation of peroxisomes, which are hybrids  
289 of mitochondrial and ER-derived precursors (Sugiura *et al.* 2017). Cellular mitochondrial  
290 homeostasis (mitostasis) is maintained through regulation at both the transcriptional and post-  
291 translational level. Cell signalling modules contribute to homeostatic regulation throughout the  
292 cell cycle or even cell death by activating proteostatic modules (*e.g.*, the ubiquitin-proteasome  
293 and autophagy-lysosome/vacuole pathways; specific proteases like LON) and genome stability  
294 modules in response to varying energy demands and stress cues (Quiros *et al.* 2016).  
295 Acetylation is a post-translational modification capable of influencing the bioenergetic  
296 response, with clinically significant implications for health and disease (Carrico *et al.* 2018).  
297 Mitochondria can traverse cell boundaries in a process known as horizontal mitochondrial  
298 transfer (Torralba *et al.* 2016).

299 Mitochondria typically maintain several copies of their own circular genome known as  
300 mitochondrial DNA (mtDNA; hundred to thousands per cell; Cummins 1998), which is  
301 maternally inherited. Biparental mitochondrial inheritance is documented in mammals, birds,  
302 fish, reptiles and invertebrate groups, and is even the norm in some bivalve taxonomic groups  
303 (Breton *et al.* 2007; White *et al.* 2008). The mitochondrial genome of the angiosperm *Amborella*  
304 contains a record of six mitochondrial genome equivalents acquired by horizontal transfer of  
305 entire genomes, two from angiosperms, three from algae and one from mosses (Rice *et al.*  
306 2016). However, some organisms such as *Cryptosporidium* species have morphologically and  
307 functionally reduced mitochondria without DNA (Liu *et al.* 2016). In vertebrates but not all  
308 invertebrates, mtDNA is compact (16.5 kB in humans) and encodes 13 protein subunits of the

309 transmembrane respiratory Complexes CI, CIII, CIV and F-ATPase, 22 tRNAs, and two RNAs.  
310 Additional gene content has been suggested to include microRNAs, piRNA, smithRNAs, repeat  
311 associated RNA, and even additional proteins (Duarte *et al.* 2014; Lee *et al.* 2015; Cobb *et al.*  
312 2016). The mitochondrial genome requires nuclear-encoded mitochondrially targeted proteins  
313 for its maintenance and expression (Rackham *et al.* 2012). Both genomes encode peptides of  
314 the membrane spanning redox pumps (CI, CIII and CIV) and F-ATPase, leading to strong  
315 constraints in the coevolution of both genomes (Blier *et al.* 2001).

316 Mitochondrial dysfunction is associated with a wide variety of genetic and degenerative  
317 diseases. Robust mitochondrial function is supported by physical exercise and caloric balance,  
318 and is central for sustained metabolic health throughout life. Therefore, a more consistent  
319 presentation of mitochondrial physiology will improve our understanding of the etiology of  
320 disease, the diagnostic repertoire of mitochondrial medicine, with a focus on protective  
321 medicine, lifestyle and healthy aging.

322 Abbreviation: mt, as generally used in mtDNA. Mitochondrion is singular and  
323 mitochondria is plural.

---

## 325 326 **1. Introduction**

327  
328 Mitochondria are the powerhouses of the cell with numerous physiological, molecular,  
329 and genetic functions (**Box 1**). Every study of mitochondrial health and disease is faced with  
330 Evolution, Age, Gender and sex, Lifestyle, and Environment (EAGLE) as essential background  
331 conditions intrinsic to the individual person or cohort, species, tissue and to some extent even  
332 cell line. As a large and coordinated group of laboratories and researchers, the mission of the  
333 global MitoEAGLE Network is to generate the necessary scale, type, and quality of consistent  
334 data sets and conditions to address this intrinsic complexity. Harmonization of experimental  
335 protocols and implementation of a quality control and data management system are required to  
336 interrelate results gathered across a spectrum of studies and to generate a rigorously monitored  
337 database focused on mitochondrial respiratory function. In this way, researchers from a variety  
338 of disciplines can compare their findings using clearly defined and accepted international  
339 standards.

340 Reliability and comparability of quantitative results depend on the accuracy of  
341 measurements under strictly-defined conditions. A conceptual framework is required to warrant  
342 meaningful interpretation and comparability of experimental outcomes carried out by research  
343 groups at different institutes. With an emphasis on quality of research, collected data can be  
344 useful far beyond the specific question of a particular experiment. Standardization and  
345 homogenization of terminology, methodology, and data sets could lead to the development of  
346 open-access databases such as those that have been developed for National Institutes of Health  
347 sponsored research in genetics, proteomics, and metabolomics. Enabling meta-analytic studies  
348 is the most economic way of providing robust answers to biological questions (Cooper *et al.*  
349 2009). Vague or ambiguous jargon can lead to confusion and may relegate valuable signals to  
350 wasteful noise. For this reason, measured values must be expressed in standard units for each  
351 parameter used to define mitochondrial respiratory function. Harmonization of nomenclature  
352 and definition of technical terms are essential to improve the awareness of the intricate meaning  
353 of current and past scientific vocabulary, for documentation and integration into databases in  
354 general, and quantitative modelling in particular (Beard 2005). The focus on coupling states  
355 and fluxes through metabolic pathways of aerobic energy transformation in mitochondrial  
356 preparations is a first step in the attempt to generate a conceptually-oriented nomenclature in  
357 bioenergetics and mitochondrial physiology. Coupling states of intact cells, the protonmotive  
358 force, and respiratory control by fuel substrates and specific inhibitors of respiratory enzymes  
359 will be reviewed in subsequent communications.

## 2. Oxidative phosphorylation and coupling states in mitochondrial preparations

‘Every professional group develops its own technical jargon for talking about matters of critical concern ... People who know a word can share that idea with other members of their group, and a shared vocabulary is part of the glue that holds people together and allows them to create a shared culture’ (Miller 1991).

**Mitochondrial preparations** are defined as either isolated mitochondria, or tissue and cellular preparations in which the barrier function of the plasma membrane is disrupted. Since this entails the loss of cell viability, mitochondrial preparations are not studied *in vivo*. In contrast to isolated mitochondria and tissue homogenate preparations, mitochondria in permeabilized tissues and cells are *in situ* relative to the plasma membrane. The plasma membrane separates the intracellular compartment including the cytosol, nucleus, and organelles from the extracellular environment. The plasma membrane consists of a lipid bilayer with embedded proteins and attached organic molecules that collectively control the selective permeability of ions, organic molecules, and particles across the cell boundary. The intact plasma membrane prevents the passage of many water-soluble mitochondrial substrates and inorganic ions—such as succinate, adenosine diphosphate (ADP) and inorganic phosphate ( $P_i$ ), that must be controlled at kinetically-saturating concentrations for the analysis of respiratory capacities. Despite of the activity of solute carriers, *e.g.*, SLC13A3 and SLC20A2, that transport these metabolites across the plasma membrane of various cell types, this limits the scope of investigations into mitochondrial respiratory function in intact cells (**Figure 2A**).

The cholesterol content of the plasma membrane is high compared to mitochondrial membranes. Therefore, mild detergents—such as digitonin and saponin—can be applied to selectively permeabilize the plasma membrane by interaction with cholesterol and allow free exchange of organic molecules and inorganic ions between the cytosol and the immediate cell environment, while maintaining the integrity and localization of organelles, cytoskeleton, and the nucleus. Application of optimum concentrations of permeabilization agents (mild detergents or toxins) leads to washout of cytosolic marker enzymes—such as lactate dehydrogenase—and results in the complete loss of cell viability, tested by nuclear staining using membrane-impermeable dyes, while mitochondrial function remains intact. Respiration of isolated mitochondria remains unaltered after the addition of low concentrations of digitonin or saponin. In addition to mechanical cell disruption during homogenization of tissue, permeabilization agents may be applied to ensure permeabilization of all cells. Suspensions of cells permeabilized in the respiration chamber and crude tissue homogenates contain all components of the cell at highly dilute concentrations. All mitochondria are retained in chemically-permeabilized mitochondrial preparations and crude tissue homogenates. In the preparation of isolated mitochondria, the cells or tissues are homogenized, and the mitochondria are separated from other cell fractions and purified by differential centrifugation, entailing the loss of a fraction of the total mitochondrial content. Typical mitochondrial recovery ranges from 30% to 80%. Using Percoll or sucrose density gradients to maximize the purity of isolated mitochondria may compromise the mitochondrial yield or structural and functional integrity. Therefore, protocols to isolate mitochondria need to be optimized according to each study. The term mitochondrial preparation does neither include further fractionation of mitochondrial components, nor submitochondrial particles.

### 2.1. Respiratory control and coupling

Respiratory coupling control states are established in studies of mitochondrial preparations to obtain reference values for various output variables (**Table 1**). Physiological conditions *in vivo* deviate from these experimentally obtained states. Since kinetically-saturating concentrations, *e.g.*, of ADP or oxygen ( $O_2$ ; dioxygen), may not apply to



411 physiological intracellular conditions, relevant information is obtained in studies of kinetic  
 412 responses to variations in [ADP] or [O<sub>2</sub>] in the range between kinetically-saturating  
 413 concentrations and anoxia (Gnaiger 2001).

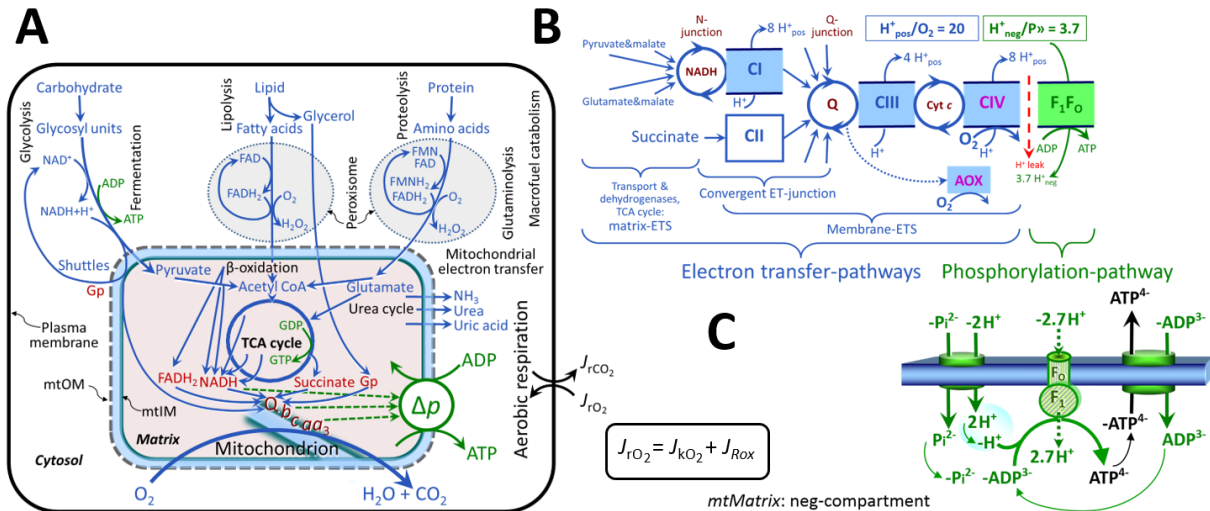
414 **The steady-state:** Mitochondria represent a thermodynamically open system in non-  
 415 equilibrium states of biochemical energy transformation. State variables (protonmotive force;  
 416 redox states) and metabolic *rates* (fluxes) are measured in defined mitochondrial respiratory  
 417 *states*. Steady-states can be obtained only in open systems, in which changes by *internal*  
 418 transformations, *e.g.*, O<sub>2</sub> consumption, are instantaneously compensated for by *external* fluxes,  
 419 *e.g.*, O<sub>2</sub> supply, preventing a change of O<sub>2</sub> concentration in the system (Gnaiger 1993b).  
 420 Mitochondrial respiratory states monitored in closed systems satisfy the criteria of pseudo-  
 421 steady states for limited periods of time, when changes in the system (concentrations of O<sub>2</sub>, fuel  
 422 substrates, ADP, P<sub>i</sub>, H<sup>+</sup>) do not exert significant effects on metabolic fluxes (respiration,  
 423 phosphorylation). Such pseudo-steady states require respiratory media with sufficient buffering  
 424 capacity and substrates maintained at kinetically-saturating concentrations, and thus depend on  
 425 the kinetics of the processes under investigation.

426 **Specification of biochemical dose:** Substrates, uncouplers, inhibitors, and other  
 427 chemical reagents are titrated to dissect mitochondrial function. Nominal concentrations of  
 428 these substances are usually reported as initial amount of substance concentration [mol·L<sup>-1</sup>] in  
 429 the incubation medium. When aiming at the measurement of kinetically saturated processes—  
 430 such as OXPHOS-capacities, the concentrations for substrates can be chosen according to the  
 431 apparent equilibrium constant,  $K_m'$ . In the case of hyperbolic kinetics, only 80% of maximum  
 432 respiratory capacity is obtained at a substrate concentration of four times the  $K_m'$ , whereas  
 433 substrate concentrations of 5, 9, 19 and 49 times the  $K_m'$  are theoretically required for reaching  
 434 83%, 90%, 95% or 98% of the maximal rate (Gnaiger 2001). Other reagents are chosen to  
 435 inhibit or alter some processes. The amount of these chemicals in an experimental incubation  
 436 is selected to maximize effect, avoiding unacceptable off-target consequences that would  
 437 adversely affect the data being sought. Specifying the amount of substance in an incubation as  
 438 nominal concentration in the aqueous incubation medium can be ambiguous (Doskey *et al.*  
 439 2015), particularly for lipophilic substances (oligomycin, uncouplers, permeabilization agents)  
 440 or cations (TPP<sup>+</sup>; fluorescent dyes such as safranin, TMRM; Chowdhury *et al.* 2015), which  
 441 accumulate in biological membranes or in the mitochondrial matrix. For example, a dose of  
 442 digitonin of 8 fmol·cell<sup>-1</sup> (10 pg·cell<sup>-1</sup>; 10 µg·10<sup>-6</sup> cells) is optimal for permeabilization of  
 443 endothelial cells, and the concentration in the incubation medium has to be adjusted according  
 444 to the cell density applied (Doerrier *et al.* 2018).

445 Generally, dose/exposure can be specified per unit of biological sample, *i.e.*, (nominal  
 446 moles of xenobiotic)/(number of cells) [mol·cell<sup>-1</sup>] or, as appropriate, per mass of biological  
 447 sample [mol·kg<sup>-1</sup>]. This approach to specification of dose/exposure provides a scalable  
 448 parameter that can be used to design experiments, help interpret a wide variety of experimental  
 449 results, and provide absolute information that allows researchers worldwide to make the most  
 450 use of published data (Doskey *et al.* 2015).

451 **Phosphorylation, P<sub>»</sub>, and P<sub>»</sub>/O<sub>2</sub> ratio:** *Phosphorylation* in the context of OXPHOS is  
 452 defined as phosphorylation of ADP by P<sub>i</sub> to form ATP. On the other hand, the term  
 453 phosphorylation is used generally in many contexts, *e.g.*, protein phosphorylation. This justifies  
 454 consideration of a symbol more discriminating and specific than P as used in the P/O ratio  
 455 (phosphate to atomic oxygen ratio), where P indicates phosphorylation of ADP to ATP or GDP  
 456 to GTP (**Figure 2**). We propose the symbol P<sub>»</sub> for the endergonic (uphill) direction of  
 457 phosphorylation ADP→ATP, and likewise the symbol P<sub>«</sub> for the corresponding exergonic  
 458 (downhill) hydrolysis ATP→ADP (**Figure 3**). P<sub>»</sub> refers mainly to electrontransfer  
 459 phosphorylation but may also involve substrate-level phosphorylation as part of the  
 460 tricarboxylic acid (TCA) cycle (succinyl-CoA ligase; phosphoglycerate kinase) and  
 461 phosphorylation of ADP catalyzed by pyruvate kinase, and of GDP phosphorylated by

462 phosphoenolpyruvate carboxykinase. Transphosphorylation is performed by adenylate kinase,  
 463 creatine kinase (mtCK), hexokinase and nucleoside diphosphate kinase. In isolated mammalian  
 464 mitochondria, ATP production catalyzed by adenylate kinase ( $2 \text{ ADP} \leftrightarrow \text{ATP} + \text{AMP}$ ) proceeds  
 465 without fuel substrates in the presence of ADP (Komlódi and Tretter 2017). Kinase cycles are  
 466 involved in intracellular energy transfer and signal transduction for regulation of energy flux.  
 467



468

469

## Figure 2. Cell respiration and oxidative phosphorylation (OXPHOS)

470

Mitochondrial respiration is the oxidation of fuel substrates (electron donors) with electron transfer to O<sub>2</sub> as the electron acceptor. For explanation of symbols see also **Figure 1**.

471

472

**(A)** Respiration of intact cells: Extra-mitochondrial catabolism of macrofuels or uptake of small molecules by the cell provides the *mitochondrial* fuel substrates. Many fuel substrates are catabolized to acetyl-CoA or to glutamate, and further electron transfer reduces nicotinamide adenine dinucleotide to NADH or flavin adenine dinucleotide to FADH<sub>2</sub>. In aerobic respiration, electron transfer is coupled to the phosphorylation of ADP to ATP, with energy transformation mediated by the protonmotive force, Δ*p*. Anabolic reactions are linked to catabolism, both by ATP as the intermediary energy currency and by small organic precursor molecules as building blocks for biosynthesis (not shown). Glycolysis involves substrate-level phosphorylation of ADP to ATP in fermentation without utilization of O<sub>2</sub>. In contrast, extra-mitochondrial oxidation of fatty acids and amino acids proceeds partially in peroxisomes without coupling to ATP production: acyl-CoA oxidase catalyzes the oxidation of FADH<sub>2</sub> with electron transfer to O<sub>2</sub>; amino acid oxidases oxidize flavin mononucleotide FMNH<sub>2</sub> or FADH<sub>2</sub>. Coenzyme Q, Q, and the cytochromes *b*, *c*, and *aa*<sub>3</sub> are redox systems of the mitochondrial inner membrane, mtIM. Dashed arrows indicate the connection between the redox proton pumps (respiratory Complexes CI, CIII and CIV) and the transmembrane Δ*p*. Mitochondrial outer membrane, mtOM; glycerol-3-phosphate, Gp; tricarboxylic acid cycle, TCA cycle.

473

474

475

476

477

478

479

480

481

482

483

484

485

486

487

488

489

**(B)** Respiration in mitochondrial preparations: The mitochondrial electron transfer system (ETS) is fuelled by diffusion and transport of substrates across the mitochondrial outer and inner membrane and consists of the matrix-ETS and membrane-ETS. ET-pathways are coupled to the phosphorylation-pathway. ET-pathways converge at the N-junction and Q-junction. Additional arrows indicate electron entry into the Q-junction through electron transferring flavoprotein, glycerophosphate dehydrogenase, dihydro-orotate dehydrogenase, choline dehydrogenase, and sulfide-ubiquinone oxidoreductase. The dotted arrow indicates the branched pathway of oxygen consumption by alternative quinol oxidase (AOX). The H<sup>+</sup><sub>pos</sub>/O<sub>2</sub> ratio is the outward proton flux from the matrix space to the positively (pos) charged vesicular compartment, divided by catabolic O<sub>2</sub> flux in the NADH-pathway. The H<sup>+</sup><sub>neg</sub>/P ratio is the inward proton flux from the inter-membrane space to the negatively (neg) charged matrix space,

498

499 divided by the flux of phosphorylation of ADP to ATP. These are not fixed stoichiometries due  
500 to ion leaks and proton slip.

501 (C) Phosphorylation-pathway catalyzed by the proton pump  $F_1F_0$ -ATPase (F-ATPase, ATP  
502 synthase), adenine nucleotide translocase, and inorganic phosphate transporter. The  $H^+_{neg}/P_{\gg}$   
503 stoichiometry is the sum of the coupling stoichiometry in the F-ATPase reaction ( $-2.7 H^+_{pos}$   
504 from the positive intermembrane space,  $2.7 H^+_{neg}$  to the matrix, *i.e.*, the negative compartment)  
505 and the proton balance in the translocation of  $ADP^{3-}$ ,  $ATP^{4-}$  and  $P_i^{2-}$ . Modified from (B)  
506 Lemieux *et al.* (2017) and (C) Gnaiger (2014).

507

508 The  $P_{\gg}/O_2$  ratio ( $P_{\gg}/4 e^-$ ) is two times the ‘P/O’ ratio ( $P_{\gg}/2 e^-$ ) of classical bioenergetics.  
509  $P_{\gg}/O_2$  is a generalized symbol, not specific for determination of  $P_i$  consumption ( $P_i/O_2$  flux  
510 ratio), ADP depletion (ADP/ $O_2$  flux ratio), or ATP production (ATP/ $O_2$  flux ratio). The  
511 mechanistic  $P_{\gg}/O_2$  ratio—or  $P_{\gg}/O_2$  stoichiometry—is calculated from the proton-to- $O_2$  and  
512 proton-to-phosphorylation coupling stoichiometries (**Figure 2B**):  
513

$$514 \quad P_{\gg}/O_2 = \frac{H^+_{pos}/O_2}{H^+_{neg}/P_{\gg}} \quad (1)$$

515

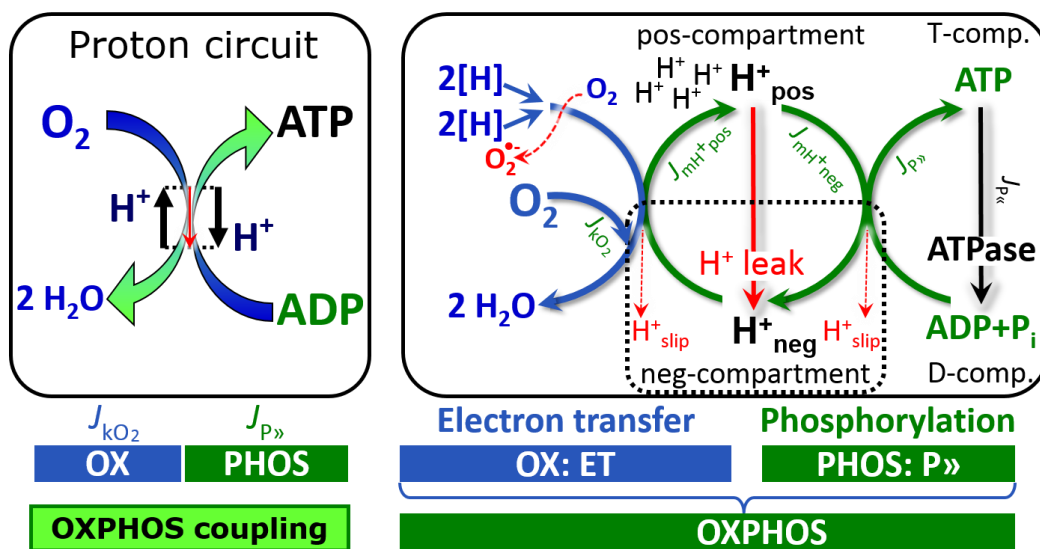
516 The  $H^+_{pos}/O_2$  coupling stoichiometry (referring to the full 4 electron reduction of  $O_2$ ) depends  
517 on the ET-pathway control state, which defines the relative involvement of the three coupling  
518 sites (respiratory Complexes I, III and IV; CI, CIII and CIV) in the catabolic pathway of  
519 electrons from the oxidation of reduced fuel substrates (electron donors) to the reduction of  $O_2$   
520 (electron acceptor). This varies with: (1) a bypass of CI by single or multiple electron input into  
521 the Q-junction; and (2) a bypass of CIV by involvement of alternative oxidases, AOX, which  
522 are not expressed in mammalian mitochondria.

523  $H^+_{pos}/O_2$  is 12 in the ET-pathways involving CIII and CIV as proton pumps, increasing to  
524 20 for the NADH-pathway through CI (**Figure 2B**), but a general consensus on  $H^+_{pos}/O_2$   
525 stoichiometries remains to be reached (Hinkle 2005; Wikström and Hummer 2012; Sazanov  
526 2015). The  $H^+_{neg}/P_{\gg}$  coupling stoichiometry (3.7; **Figure 2B**) is the sum of 2.7  $H^+_{neg}$  required  
527 by the F-ATPase of vertebrate and most invertebrate species (Watt *et al.* 2010) and the proton  
528 balance in the translocation of ADP, ATP and  $P_i$  (**Figure 2C**). Taken together, the mechanistic  
529  $P_{\gg}/O_2$  ratio is calculated at 5.4 and 3.3 for NADH- and succinate-linked respiration, respectively  
530 (Eq. 1). The corresponding classical  $P_{\gg}/O$  ratios (referring to the 2 electron reduction of  $0.5 O_2$ )  
531 are 2.7 and 1.6 (Watt *et al.* 2010), in agreement with the measured  $P_{\gg}/O$  ratio for succinate of  
532  $1.58 \pm 0.02$  (Gnaiger *et al.* 2000).

533 The effective  $P_{\gg}/O_2$  flux ratio ( $Y_{P_{\gg}/O_2} = J_{P_{\gg}}/J_{kO_2}$ ; **Figure 3**) is diminished relative to the  
534 mechanistic  $P_{\gg}/O_2$  ratio by intrinsic and extrinsic uncoupling and dyscoupling (**Figure 4**). Such  
535 generalized uncoupling is different from switching to mitochondrial pathways that involve  
536 fewer than three proton pumps (‘coupling sites’: Complexes CI, CIII and CIV), bypassing CI  
537 through multiple electron entries into the Q-junction, or CIII and CIV through AOX (**Figure**  
538 **2B**). Reprogramming of mitochondrial pathways leading to different types of substrates being  
539 oxidized may be considered as a switch of gears (changing the stoichiometry by altering the  
540 substrate that is oxidized) rather than uncoupling (loosening the tightness of coupling relative  
541 to a fixed stoichiometry). In addition,  $Y_{P_{\gg}/O_2}$  depends on several experimental conditions of flux  
542 control, increasing as a hyperbolic function of [ADP] to a maximum value (Gnaiger 2001).

543 **Control and regulation:** The terms metabolic *control* and *regulation* are frequently used  
544 synonymously, but are distinguished in metabolic control analysis: ‘We could understand the  
545 regulation as the mechanism that occurs when a system maintains some variable constant over  
546 time, in spite of fluctuations in external conditions (homeostasis of the internal state). On the  
547 other hand, metabolic control is the power to change the state of the metabolism in response to  
548 an external signal’ (Fell 1997). Respiratory control may be induced by experimental control  
549 signals that *exert* an influence on: (1) ATP demand and ADP phosphorylation-rate; (2) fuel

550 substrate composition, pathway competition; (3) available amounts of substrates and  $O_2$ , *e.g.*,  
 551 starvation and hypoxia; (4) the protonmotive force, redox states, flux–force relationships,  
 552 coupling and efficiency; (5)  $Ca^{2+}$  and other ions including  $H^+$ ; (6) inhibitors, *e.g.*, nitric oxide  
 553 or intermediary metabolites such as oxaloacetate; (7) signalling pathways and regulatory  
 554 proteins, *e.g.*, insulin resistance, transcription factor hypoxia inducible factor 1. *Mechanisms* of  
 555 respiratory control and regulation include adjustments of: (1) enzyme activities by allosteric  
 556 mechanisms and phosphorylation; (2) enzyme content, concentrations of cofactors and  
 557 conserved moieties—such as adenylates, nicotinamide adenine dinucleotide [ $NAD^+/NADH$ ],  
 558 coenzyme Q, cytochrome *c*; (3) metabolic channeling by supercomplexes; and (4)  
 559 mitochondrial density (enzyme concentrations and membrane area) and morphology (cristae  
 560 folding, fission and fusion). Mitochondria are targeted directly by hormones, thereby affecting  
 561 their energy metabolism (Lee *et al.* 2013; Gerö and Szabo 2016; Price and Dai 2016; Moreno  
 562 *et al.* 2017). Evolutionary or acquired differences in the genetic and epigenetic basis of  
 563 mitochondrial function (or dysfunction) between individuals; age; gender, biological sex, and  
 564 hormone concentrations; life style including exercise and nutrition; and environmental issues  
 565 including thermal, atmospheric, toxic and pharmacological factors, exert an influence on all  
 566 control mechanisms listed above. For reviews, see Brown 1992; Gnaiger 1993a, 2009; 2014;  
 567 Paradies *et al.* 2014; Morrow *et al.* 2017.



569 **Figure 3. Coupling in oxidative phosphorylation (OXPHOS)**

570  $2[H]$  indicates the reduced hydrogen equivalents of fuel substrates of the catabolic reaction  $k$   
 571 with oxygen.  $O_2$  flux,  $J_{kO_2}$ , through the catabolic ET-pathway, is coupled to flux through the  
 572 phosphorylation-pathway of ADP to ATP,  $J_{P\gg}$ . The redox proton pumps of the ET-pathway  
 573 drive proton flux into the positive (pos) compartment,  $J_{mH^+pos}$ , generating the output  
 574 protonmotive force (motive, subscript  $m$ ). F-ATPase is coupled to inward proton current into  
 575 the negative (neg) compartment,  $J_{mH^+neg}$ , to phosphorylate ADP to ATP. The system is defined  
 576 by the boundaries (full black line) and is not a black box, but is analysed as a compartmental  
 577 system. The negative compartment (neg-compartment, enclosed by the dotted line) is the  
 578 matrix space, separated by the mtIM from the positive compartment (pos-compartment).  
 579  $ADP+P_i$  and ATP are the substrate- and product-compartments (scalar ADP and ATP  
 580 compartments, D-comp. and T-comp.), respectively. At steady-state proton turnover,  $J_{\infty H^+}$ , and  
 581 ATP turnover,  $J_{\infty P}$ , maintain concentrations constant, when  $J_{mH^+\infty} = J_{mH^+pos} = J_{mH^+neg}$ , and  
 582  $J_{P\gg} = J_{P\ll}$ . Modified from Gnaiger (2014).

583

584 **Respiratory control and response:** Lack of control by a metabolic pathway, *e.g.*,  
 585 phosphorylation-pathway, means that there will be no response to a variable activating it, *e.g.*,

586 [ADP]. The reverse, however, is not true as the absence of a response to [ADP] does not exclude  
 587 the phosphorylation-pathway from having some degree of control. The degree of control of a  
 588 component of the OXPHOS-pathway on an output variable—such as O<sub>2</sub> flux, will in general  
 589 be different from the degree of control on other outputs—such as phosphorylation-flux or  
 590 proton leak flux. Therefore, it is necessary to be specific as to which input and output are under  
 591 consideration (Fell 1997).

592 **Respiratory coupling control and ET-pathway control:** Respiratory control refers to  
 593 the ability of mitochondria to adjust O<sub>2</sub> flux in response to external control signals by engaging  
 594 various mechanisms of control and regulation. Respiratory control is monitored in a  
 595 mitochondrial preparation under conditions defined as respiratory states. When  
 596 phosphorylation of ADP to ATP is stimulated or depressed, an increase or decrease is observed  
 597 in electron transfer measured as O<sub>2</sub> flux in respiratory coupling states of intact mitochondria  
 598 ('controlled states' in the classical terminology of bioenergetics). Alternatively, coupling of  
 599 electron transfer with phosphorylation is disengaged by uncouplers. These protonophores are  
 600 weak lipid-soluble acids which disrupt the barrier function of the mtIM and thus shortcircuit  
 601 the protonmotive system, functioning like a clutch in a mechanical system. The corresponding  
 602 coupling control state is characterized by a high O<sub>2</sub> flux without control by P» ('uncontrolled  
 603 state').

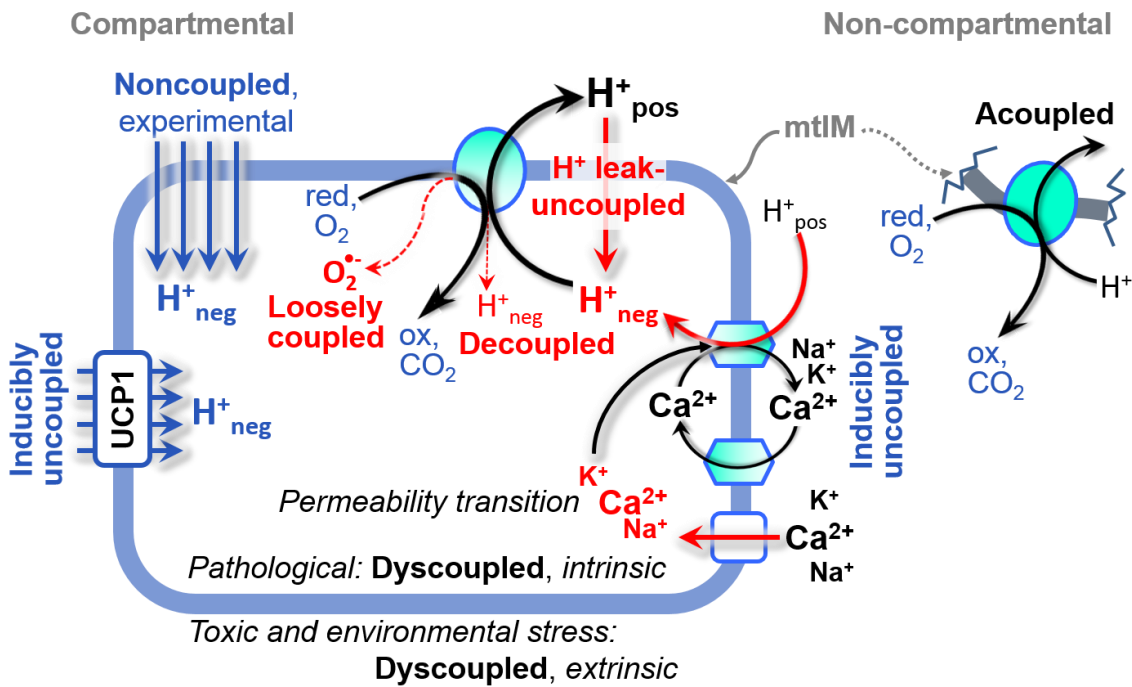
604 ET-pathway control states are obtained in mitochondrial preparations by depletion of  
 605 endogenous substrates and addition to the mitochondrial respiration medium of fuel substrates  
 606 (2[H] in **Figure 3**) and specific inhibitors, activating selected mitochondrial catabolic pathways,  
 607 k, of electron transfer from the oxidation of fuel substrates to reduction of O<sub>2</sub> (**Figure 2A**).  
 608 Coupling control states and pathway control states are complementary, since mitochondrial  
 609 preparations depend on an exogenous supply of pathway-specific fuel substrates and oxygen  
 610 (Gnaiger 2014).

611 **Coupling:** In mitochondrial electron transfer, vectorial transmembrane proton flux is  
 612 coupled through the redox proton pumps CI, CIII and CIV to the catabolic flux of scalar  
 613 reactions, collectively measured as O<sub>2</sub> flux (**Figure 3**). Thus mitochondria are elements of  
 614 energy transformation. Energy is a conserved quantity and cannot be lost or produced in any  
 615 internal process (First Law of thermodynamics). Open and closed systems can gain or lose  
 616 energy only by external fluxes—by exchange with the environment. Therefore, energy can  
 617 neither be produced by mitochondria, nor is there any internal process without energy  
 618 conservation. Exergy or Gibbs energy ('free energy') is the part of energy that can potentially  
 619 be transformed into work under conditions of constant volume and pressure. *Coupling* is the  
 620 interaction of an exergonic process (spontaneous, negative exergy change) with an endergonic  
 621 process (positive exergy change) in energy transformations which conserve part of the exergy  
 622 that would be irreversibly lost or dissipated in an uncoupled process.

623 **Uncoupling:** Uncoupling of mitochondrial respiration is a general term comprising  
 624 diverse mechanisms:

- 625 1. Proton leak across the mtIM from the pos- to the neg-compartment (**Figure 3**);
- 626 2. Cycling of other cations, strongly stimulated by permeability transition, or  
 627 experimentally induced by valinomycin in the presence of K<sup>+</sup>;
- 628 3. Proton slip in the redox proton pumps when protons are effectively not pumped (CI,  
 629 CIII and CIV) or are not driving phosphorylation (F-ATPase);
- 630 4. Loss of vesicular (compartmental) integrity when electron transfer is acoupled;
- 631 5. Electron leak in the loosely coupled univalent reduction of O<sub>2</sub> to superoxide (O<sub>2</sub><sup>•-</sup>;  
 632 superoxide anion radical).

633 Differences of terms—uncoupled vs. noncoupled—are easily overlooked, although they relate  
 634 to different meanings of uncoupling (**Figure 4** and **Table 2**).



635  
636  
637  
638  
639  
640  
641  
642  
643  
644  
645  
646  
647  
648

#### Figure 4. Mechanisms of respiratory uncoupling

An intact mitochondrial inner membrane, mtIM, is required for vectorial, compartmental coupling. ‘Acoupled’ respiration is the consequence of structural disruption with catalytic activity of non-compartmental mitochondrial fragments. Inducibly uncoupled (activation of UCP1) and experimentally noncoupled respiration (titration of protonophores) stimulate respiration to maximum O<sub>2</sub> flux. H<sup>+</sup> leak-uncoupled, decoupled, and loosely coupled respiration are components of intrinsic uncoupling. Pathological dysfunction may affect all types of uncoupling, including permeability transition, causing intrinsically dyscoupled respiration. Similarly, toxicological and environmental stress factors can cause extrinsically dyscoupled respiration.

#### 2.2. Coupling states and respiratory rates

649  
650  
651  
652  
653  
654  
655  
656  
657  
658

**Respiratory capacities in coupling control states:** To extend the classical nomenclature on mitochondrial coupling states (Section 2.3) by a concept-driven terminology that explicitly incorporates information on the meaning of respiratory states, the terminology must be general and not restricted to any particular experimental protocol or mitochondrial preparation (Gnaiger 2009). Concept-driven nomenclature aims at mapping the *meaning and concept behind* the words and acronyms onto the *forms* of words and acronyms (Miller 1991). The focus of concept-driven nomenclature is primarily the conceptual ‘why’, along with clarification of the experimental ‘how’. Respiratory capacities delineate, comparable to channel capacity in information theory (Schneider 2006), the upper bound of the rate of respiration measured in defined coupling control states and electron transfer-pathway (ET-pathway) states (Figure 5).

659  
660  
661  
662  
663  
664  
665  
666  
667

To provide a diagnostic reference for respiratory capacities of core energy metabolism, the capacity of *oxidative phosphorylation*, OXPHOS, is measured at kinetically-saturating concentrations of ADP and P<sub>i</sub>. The *oxidative ET-capacity* reveals the limitation of OXPHOS-capacity mediated by the *phosphorylation-pathway*. The ET- and phosphorylation-pathways comprise coupled segments of the OXPHOS-system. ET-capacity is measured as noncoupled respiration by application of *external uncouplers*. The contribution of *intrinsically uncoupled* O<sub>2</sub> consumption is studied by preventing the stimulation of phosphorylation either in the absence of ADP or by inhibition of the phosphorylation-pathway. The corresponding states are collectively classified as LEAK-states, when O<sub>2</sub> consumption compensates mainly for ion

668 leaks, including the proton leak. Defined coupling states are induced by: (1) adding cation  
 669 chelators such as EGTA, binding free  $\text{Ca}^{2+}$  and thus limiting cation cycling; (2) adding ADP  
 670 and  $\text{P}_i$ ; (3) inhibiting the phosphorylation-pathway; and (4) uncoupler titrations, while  
 671 maintaining a defined ET-pathway state with constant fuel substrates and inhibitors of specific  
 672 branches of the ET-pathway (**Figure 5**).

673

674 **Figure 5. Four-compartment model of oxidative phosphorylation**

675 Respiratory states (ET, OXPHOS, LEAK; **Table 1**) and corresponding rates ( $E$ ,  $P$ ,  $L$ ) are  
 676 connected by the protonmotive force,  $\Delta p$ . ET-capacity,  $E$  ( $I$ ), is  
 677 partitioned into (2) dissipative LEAK-respiration,  $L$ , when the  
 678 Gibbs energy change of catabolic

680  $\text{O}_2$  flux is irreversibly lost, (3) net OXPHOS-capacity,  $P-L$ , with partial conservation of the  
 681 capacity to perform work, and (4) the excess capacity,  $E-P$ . Modified from Gnaiger (2014).

682

683 **Table 1. Coupling states and residual oxygen consumption in mitochondrial preparations in relation to respiration- and phosphorylation-flux,  $J_{\text{KO}_2}$  and  $J_{\text{P}}$ , and protonmotive force,  $\Delta p$ .** Coupling states are established at kinetically-saturating concentrations of fuel substrates and  $\text{O}_2$ .

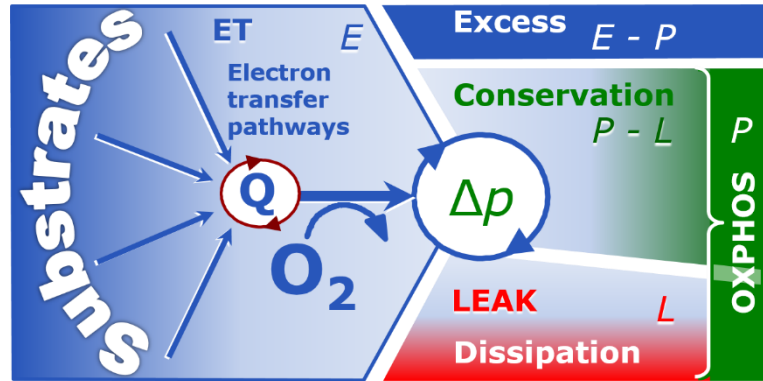
684

685

State	$J_{\text{KO}_2}$	$J_{\text{P}}$	$\Delta p$	Inducing factors	Limiting factors
LEAK	$L$ ; low, cation leak-dependent respiration	0	max.	back-flux of cations including proton leak, proton slip	$J_{\text{P}} = 0$ : (1) without ADP, $L_N$ ; (2) max. ATP/ADP ratio, $L_T$ ; or (3) inhibition of the phosphorylation-pathway, $L_{\text{Omy}}$
OXPHOS	$P$ ; high, ADP-stimulated respiration	max.	high	kinetically-saturating [ADP] and [ $\text{P}_i$ ]	$J_{\text{P}}$ , by phosphorylation-pathway; or $J_{\text{KO}_2}$ by ET-capacity
ET	$E$ ; max., noncoupled respiration	0	low	optimal external uncoupler concentration for max. $J_{\text{O}_2, E}$	$J_{\text{KO}_2}$ by ET-capacity
ROX	$R_{\text{ox}}$ ; min., residual $\text{O}_2$ consumption	0	0	$J_{\text{O}_2, R_{\text{ox}}}$ in non-ET-pathway oxidation reactions	inhibition of all ET-pathways; or absence of fuel substrates

692

693 The three coupling states, ET, LEAK and OXPHOS, are shown schematically with the  
 694 corresponding respiratory rates, abbreviated as  $E$ ,  $L$  and  $P$ , respectively (**Figure 5**). We  
 695 distinguish metabolic *pathways* from metabolic *states* and the corresponding metabolic *rates*;  
 696 for example: ET-pathways (**Figure 5**), ET-states (**Figure 6C**), and ET-capacities,  $E$ ,  
 697 respectively (**Table 1**). The protonmotive force is *high* in the OXPHOS-state when it drives  
 698 phosphorylation, *maximum* in the LEAK-state of coupled mitochondria, driven by LEAK-



699 respiration at a minimum back-  
 700 flux of cations to the matrix  
 701 side, and *very low* in the ET-  
 702 state when uncouplers short-  
 703 circuit the proton cycle (**Table**  
 704 **1**).

705 **LEAK-state** (**Figure**  
 706 **6A**): The LEAK-state is defined  
 707 as a state of mitochondrial  
 708 respiration when  $O_2$  flux mainly  
 709 compensates for ion leaks in the  
 710 absence of ATP synthesis, at  
 711 kinetically-saturating  
 712 concentrations of  $O_2$  and  
 713 respiratory fuel substrates.  
 714 LEAK-respiration is measured  
 715 to obtain an estimate of *intrinsic*  
 716 *uncoupling* without addition of  
 717 an experimental uncoupler: (1)  
 718 in the absence of adenylates,  
 719 *i.e.*, AMP, ADP and ATP; (2)  
 720 after depletion of ADP at a  
 721 maximum ATP/ADP ratio; or  
 722 (3) after inhibition of the  
 723 phosphorylation-pathway by  
 724 inhibitors of F-ATPase—such  
 725 as oligomycin, or of adenine  
 726 nucleotide translocase—such as  
 727 carboxyatractyloside.

728 Adjustment of the nominal  
 729 concentration of these inhibitors  
 730 to the density of biological  
 731 sample applied can minimize or  
 732 avoid inhibitory side-effects  
 733 exerted on ET-capacity or even  
 734 some dyscoupling.

735 **Proton leak and**  
 736 **uncoupled respiration:** Proton  
 737 leak is a leak current of protons.  
 738 The intrinsic proton leak is the  
 739 *uncoupled* process in which  
 740 protons diffuse across the mtIM  
 741 in the dissipative direction of the  
 742 downhill protonmotive force  
 743 without coupling to phosphorylation (**Figure 6A**). The proton leak flux depends non-linearly  
 744 on the protonmotive force (Garlid *et al.* 1989; Divakaruni and Brand 2011), it is a property of  
 745 the mtIM and may be enhanced due to possible contaminations by free fatty acids. Inducible  
 746 uncoupling mediated by uncoupling protein 1 (UCP1) is physiologically controlled, *e.g.*, in  
 747 brown adipose tissue. UCP1 is a member of the mitochondrial carrier family that is involved in  
 748 the translocation of protons across the mtIM (Klingenberg 2017). Consequently, the short-

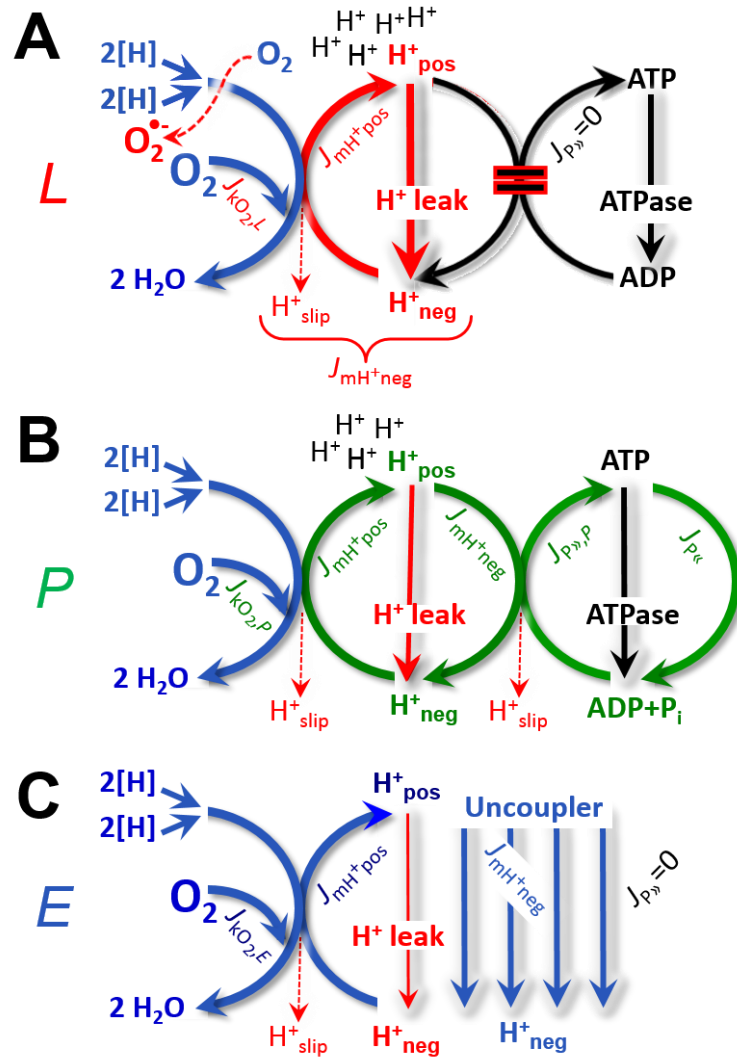


**Figure 6. Respiratory coupling states**

(A) **LEAK-state and rate, L:** Phosphorylation is arrested,  $J_{P_{\gg}} = 0$ , and catabolic  $O_2$  flux,  $J_{kO_2,L}$ , is controlled mainly by the proton leak,  $J_{mH^{+}neg,L}$ , at maximum protonmotive force (**Figure 4**).

(B) **OXPHOS-state and rate, P:** Phosphorylation,  $J_{P_{\gg}}$ , is stimulated by kinetically-saturating [ADP] and  $[P_i]$ , and is supported by a high protonmotive force.  $O_2$  flux,  $J_{kO_2,P}$ , is well-coupled at a  $P_{\gg}/O_2$  ratio of  $J_{P_{\gg},P}/J_{O_2,P}$ .

(C) **ET-state and rate, E:** Noncoupled respiration,  $J_{kO_2,E}$ , is maximum at optimum exogenous uncoupler concentration and phosphorylation is zero,  $J_{P_{\gg}} = 0$ . See also **Figure 3**.



749 circuit diminishes the protonmotive force and stimulates electron transfer to O<sub>2</sub> and heat  
750 dissipation without phosphorylation of ADP.

751 **Cation cycling:** There can be other cation contributors to leak current including calcium  
752 and probably magnesium. Calcium influx is balanced by mitochondrial Na<sup>+</sup>/Ca<sup>2+</sup> or H<sup>+</sup>/Ca<sup>2+</sup>  
753 exchange, which is balanced by Na<sup>+</sup>/H<sup>+</sup> or K<sup>+</sup>/H<sup>+</sup> exchanges. This is another effective  
754 uncoupling mechanism different from proton leak (**Table 2**).

755

756 **Table 2. Terms on respiratory coupling and uncoupling.**

Term	$J_{kO_2}$	$P \gg O_2$	Note	
acoupled		0	electron transfer in mitochondrial fragments without vectorial proton translocation ( <b>Figure 4</b> )	
intrinsic, no protonophore added	uncoupled	$L$	0	non-phosphorylating LEAK-respiration ( <b>Figure 6A</b> )
	proton leak-uncoupled		0	component of $L$ , H <sup>+</sup> diffusion across the mtIM ( <b>Figure 4</b> )
	decoupled		0	component of $L$ , proton slip ( <b>Figure 4</b> )
	loosely coupled		0	component of $L$ , lower coupling due to superoxide formation and bypass of proton pumps ( <b>Figure 4</b> )
	dyscoupled		0	pathologically, toxicologically, environmentally increased uncoupling, mitochondrial dysfunction
	inducibly uncoupled		0	by UCP1 or cation ( <i>e.g.</i> , Ca <sup>2+</sup> ) cycling ( <b>Figure 4</b> )
noncoupled	$E$	0	non-phosphorylating respiration stimulated to maximum flux at optimum exogenous uncoupler concentration ( <b>Figure 6C</b> )	
well-coupled	$P$	high	phosphorylating respiration with an intrinsic LEAK component ( <b>Figure 6B</b> )	
fully coupled	$P - L$	max.	OXPPOS-capacity corrected for LEAK-respiration ( <b>Figure 5</b> )	

757

758 **Proton slip and decoupled respiration:** Proton slip is the *decoupled* process in which  
759 protons are only partially translocated by a redox proton pump of the ET-pathways and slip  
760 back to the original vesicular compartment. The proton leak is the dominant contributor to the  
761 overall leak current in mammalian mitochondria incubated under physiological conditions at  
762 37 °C, whereas proton slip is increased at lower experimental temperature (Canton *et al.* 1995).  
763 Proton slip can also happen in association with the F-ATPase, in which the proton slips downhill  
764 across the pump to the matrix without contributing to ATP synthesis. In each case, proton slip  
765 is a property of the proton pump and increases with the pump turnover rate.

766 **Electron leak and loosely coupled respiration:** Superoxide production by the ETS leads  
767 to a bypass of redox proton pumps and correspondingly lower  $P \gg O_2$  ratio. This depends on the  
768 actual site of electron leak and the scavenging of hydrogen peroxide by cytochrome *c*, whereby  
769 electrons may re-enter the ETS with proton translocation by CIV.

770 **Loss of compartmental integrity and acoupled respiration:** Electron transfer and  
771 catabolic O<sub>2</sub> flux proceed without compartmental proton translocation in disrupted  
772 mitochondrial fragments. Such fragments form during mitochondrial isolation, and may not  
773 fully fuse to re-establish structurally intact mitochondria. Loss of mtIM integrity, therefore, is

774 the cause of acoupled respiration, which is a nonvectorial dissipative process without control  
775 by the protonmotive force.

776 **Dyscoupled respiration:** Mitochondrial injuries may lead to *dyscoupling* as a  
777 pathological or toxicological cause of *uncoupled* respiration. Dyscoupling may involve any  
778 type of uncoupling mechanism, *e.g.*, opening the permeability transition pore. Dyscoupled  
779 respiration is distinguished from the experimentally induced *noncoupled* respiration in the ET-  
780 state (**Table 2**).

781 **OXPHOS-state (Figure 6B):** The OXPHOS-state is defined as the respiratory state with  
782 kinetically-saturating concentrations of O<sub>2</sub>, respiratory and phosphorylation substrates, and  
783 absence of exogenous uncoupler, which provides an estimate of the maximal respiratory  
784 capacity in the OXPHOS-state for any given ET-pathway state. Respiratory capacities at  
785 kinetically-saturating substrate concentrations provide reference values or upper limits of  
786 performance, aiming at the generation of data sets for comparative purposes. Physiological  
787 activities and effects of substrate kinetics can be evaluated relative to the OXPHOS-capacity.

788 As discussed previously, 0.2 mM ADP does not fully saturate flux in isolated  
789 mitochondria (Gnaiger 2001; Puchowicz *et al.* 2004); greater ADP concentration is required,  
790 particularly in permeabilized muscle fibres and cardiomyocytes, to overcome limitations by  
791 intracellular diffusion and by the reduced conductance of the mtOM (Jepihhina *et al.* 2011,  
792 Illaste *et al.* 2012, Simson *et al.* 2016), either through interaction with tubulin (Rostovtseva *et al.*  
793 2008) or other intracellular structures (Birkedal *et al.* 2014). In addition, saturating ADP  
794 concentrations need to be evaluated under different experimental conditions such as  
795 temperature (Lemieux *et al.* 2017) and with different animal models (Blier and Guderley, 1993).  
796 In permeabilized muscle fibre bundles of high respiratory capacity, the apparent  $K_m$  for ADP  
797 increases up to 0.5 mM (Saks *et al.* 1998), consistent with experimental evidence that >90%  
798 saturation is reached only at >5 mM ADP (Pesta and Gnaiger 2012). Similar ADP  
799 concentrations are also required for accurate determination of OXPHOS-capacity in human  
800 clinical cancer samples and permeabilized cells (Klepinin *et al.* 2016; Koit *et al.* 2017).  
801 Whereas 2.5 to 5 mM ADP is sufficient to obtain the actual OXPHOS-capacity in many types  
802 of permeabilized tissue and cell preparations, experimental validation is required in each  
803 specific case.

804 **Electron transfer-state (Figure 6C):** O<sub>2</sub> flux determined in the ET-state yields an  
805 estimate of ET-capacity. The ET-state is defined as the *noncoupled* state with kinetically-  
806 saturating concentrations of O<sub>2</sub>, respiratory substrate and optimum *exogenous* uncoupler  
807 concentration for maximum O<sub>2</sub> flux. As a consequence of the nearly collapsed protonmotive  
808 force, the driving force is insufficient for phosphorylation, and  $J_{P_{\gg}} = 0$ . The most frequently  
809 used uncouplers are carbonyl cyanide *m*-chloro phenyl hydrazone, carbonyl cyanide *p*-  
810 trifluoromethoxyphenylhydrazone or dinitrophenol (CCCP, FCCP, DNP). Stepwise titration  
811 of uncouplers stimulates respiration up to or above the level of O<sub>2</sub> consumption rates in the  
812 OXPHOS-state, but inhibition of respiration is observed above optimum uncoupler  
813 concentrations (Mitchell 2011). Data obtained with a single dose of uncoupler must be  
814 evaluated with caution, particularly when a fixed uncoupler concentration is used in studies  
815 exploring a treatment or disease that may alter the mitochondrial content or mitochondrial  
816 sensitivity to inhibition by uncouplers.

817 **ROX state and Rox:** Besides the three fundamental coupling states of mitochondrial  
818 preparations, the state of residual O<sub>2</sub> consumption, ROX, is relevant to assess respiratory  
819 function (**Figure 1**). ROX is not a coupling state. The rate of residual oxygen consumption,  
820 *Rox*, is defined as O<sub>2</sub> consumption due to oxidative reactions measured after inhibition of ET—  
821 with rotenone, malonic acid and antimycin A. Cyanide and azide inhibit not only CIV but  
822 catalase and several peroxidases involved in *Rox*. However, high concentrations of antimycin  
823 A, but not rotenone or cyanide, inhibit peroxisomal acyl-CoA oxidase and D-amino acid  
824 oxidase (Vamecq *et al.* 1987). ROX represents a baseline that is used to correct respiration

825 measured in defined coupling states. *Rox*-corrected  $L$ ,  $P$  and  $E$  not only lower the values of total  
 826 fluxes, but also changes the flux control ratios  $L/P$  and  $L/E$ . *Rox* is not necessarily equivalent  
 827 to non-mitochondrial reduction of  $O_2$ , considering  $O_2$ -consuming reactions in mitochondria that  
 828 are not related to ET—such as  $O_2$  consumption in reactions catalyzed by monoamine oxidases  
 829 (type A and B), monooxygenases (cytochrome P450 monooxygenases), dioxygenase (sulfur  
 830 dioxygenase and trimethyllysine dioxygenase), and several hydroxylases. Even isolated  
 831 mitochondrial fractions, especially those obtained from liver, may be contaminated by  
 832 peroxisomes. This fact makes the exact determination of mitochondrial  $O_2$  consumption and  
 833 mitochondria-associated generation of reactive oxygen species complicated (Schönfeld *et al.*  
 834 2009; Speijer 2016; **Figure 2**). The dependence of ROX-linked  $O_2$  consumption needs to be  
 835 studied in detail together with non-ET enzyme activities, availability of specific substrates,  $O_2$   
 836 concentration, and electron leakage leading to the formation of reactive oxygen species.

837 **Quantitative relations:**  $E$  may exceed or be equal to  $P$ .  $E > P$  is observed in many types  
 838 of mitochondria, varying between species, tissues and cell types (Gnaiger 2009).  $E-P$  is the  
 839 excess ET-capacity pushing the phosphorylation-flux (**Figure 2C**) to the limit of its *capacity of*  
 840 *utilizing* the protonmotive force. In addition, the magnitude of  $E-P$  depends on the tightness of  
 841 respiratory coupling or degree of uncoupling, since an increase of  $L$  causes  $P$  to increase  
 842 towards the limit of  $E$ . The *excess*  $E-P$  capacity,  $E-P$ , therefore, provides a sensitive diagnostic  
 843 indicator of specific injuries of the phosphorylation-pathway, under conditions when  $E$  remains  
 844 constant but  $P$  declines relative to controls (**Figure 5**). Substrate cocktails supporting  
 845 simultaneous convergent electron transfer to the Q-junction for reconstitution of TCA cycle  
 846 function establish pathway control states with high ET-capacity, and consequently increase the  
 847 sensitivity of the  $E-P$  assay.

848  $E$  cannot theoretically be lower than  $P$ .  $E < P$  must be discounted as an artefact, which  
 849 may be caused experimentally by: (1) loss of oxidative capacity during the time course of the  
 850 respirometric assay, since  $E$  is measured subsequently to  $P$ ; (2) using insufficient uncoupler  
 851 concentrations; (3) using high uncoupler concentrations which inhibit ET (Gnaiger 2008); (4)  
 852 high oligomycin concentrations applied for measurement of  $L$  before titrations of uncoupler,  
 853 when oligomycin exerts an inhibitory effect on  $E$ . On the other hand, the excess ET-capacity is  
 854 overestimated if non-saturating [ADP] or  $[P_i]$  are used. See State 3 in the next section.

855 The net OXPHOS-capacity is calculated by subtracting  $L$  from  $P$  (**Figure 5**). The net  
 856  $P \gg O_2$  equals  $P \gg (P-L)$ , wherein the dissipative LEAK component in the OXPHOS-state may  
 857 be overestimated. This can be avoided by measuring LEAK-respiration in a state when the  
 858 protonmotive force is adjusted to its slightly lower value in the OXPHOS-state—by titration of  
 859 an ET inhibitor (Divakaruni and Brand 2011). Any turnover-dependent components of proton  
 860 leak and slip, however, are underestimated under these conditions (Garlid *et al.* 1993). In  
 861 general, it is inappropriate to use the term *ATP production* or *ATP turnover* for the difference  
 862 of  $O_2$  flux measured in the OXPHOS and LEAK states.  $P-L$  is the upper limit of OXPHOS-  
 863 capacity that is freely available for ATP production (corrected for LEAK-respiration) and is  
 864 fully coupled to phosphorylation with a maximum mechanistic stoichiometry (**Figure 5**).

865 The rates of LEAK respiration and OXPHOS capacity depend on (1) the tightness of  
 866 coupling under the influence of the respiratory uncoupling mechanisms (**Figure 4**), and (2) the  
 867 coupling stoichiometry, which varies as a function of the substrate type undergoing oxidation  
 868 in ET-pathways with either two or three coupling sites (**Figure 2B**). When cocktails with  
 869 NADH-linked substrates and succinate are used, the relative contribution of ET-pathways with  
 870 three or two coupling sites cannot be controlled experimentally, is difficult to determine, and  
 871 may shift in transitions between LEAK-, OXPHOS- and ET-states (Gnaiger 2014). Under these  
 872 experimental conditions, we cannot separate the tightness of coupling *versus* coupling  
 873 stoichiometry as the mechanisms of respiratory control in the shift of  $L/P$  ratios. The tightness  
 874 of coupling and fully coupled  $O_2$  flux,  $P-L$  (**Table 2**), therefore, are obtained from  
 875 measurements of coupling control of LEAK respiration, OXPHOS- and ET-capacities in well

876 defined pathway states, using either pyruvate and malate as substrates or the classical succinate  
877 and rotenone substrate-inhibitor combination (**Figure 2B**).

878

### 879 2.3. Classical terminology for isolated mitochondria

880 'When a code is familiar enough, it ceases appearing like a code; one forgets that there  
881 is a decoding mechanism. The message is identical with its meaning' (Hofstadter 1979).

882

883 Chance and Williams (1955; 1956) introduced five classical states of mitochondrial  
884 respiration and cytochrome redox states. **Table 3** shows a protocol with isolated mitochondria  
885 in a closed respirometric chamber, defining a sequence of respiratory states. States and rates  
886 are not specifically distinguished in this nomenclature.

887

888

889

**Table 3. Metabolic states of mitochondria (Chance and Williams, 1956; Table V).**

State	[O <sub>2</sub> ]	ADP level	Substrate Level	Respiration rate	Rate-limiting substance
1	>0	low	Low	slow	ADP
2	>0	high	~0	slow	substrate
3	>0	high	high	fast	respiratory chain
4	>0	low	high	slow	ADP
5	0	high	high	0	oxygen

891

892 **State 1** is obtained after addition of isolated mitochondria to air-saturated  
893 isoosmotic/isotonic respiration medium containing P<sub>i</sub>, but no fuel substrates and no adenylates,  
894 *i.e.*, AMP, ADP, ATP.

895 **State 2** is induced by addition of a 'high' concentration of ADP (typically 100 to 300  
896 μM), which stimulates respiration transiently on the basis of endogenous fuel substrates and  
897 phosphorylates only a small portion of the added ADP. State 2 is then obtained at a low  
898 respiratory activity limited by exhausted endogenous fuel substrate availability (**Table 3**). If  
899 addition of specific inhibitors of respiratory complexes—such as rotenone—does not cause a  
900 further decline of O<sub>2</sub> flux, State 2 is equivalent to the ROX state (See below.). If inhibition is  
901 observed, undefined endogenous fuel substrates are a confounding factor of pathway control,  
902 contributing to the effect of subsequently externally added substrates and inhibitors. In contrast  
903 to the original protocol, an alternative sequence of titration steps is frequently applied, in which  
904 the alternative 'State 2' has an entirely different meaning, when this second state is induced by  
905 addition of fuel substrate without ADP (LEAK-state; in contrast to State 2 defined in **Table 1**  
906 as a ROX state), followed by addition of ADP.

907 **State 3** is the state stimulated by addition of fuel substrates while the ADP concentration  
908 is still high (**Table 3**) and supports coupled energy transformation through oxidative  
909 phosphorylation. 'High ADP' is a concentration of ADP specifically selected to allow the  
910 measurement of State 3 to State 4 transitions of isolated mitochondria in a closed respirometric  
911 chamber. Repeated ADP titration re-establishes State 3 at 'high ADP'. Starting at O<sub>2</sub>  
912 concentrations near air-saturation (ca. 200 μM O<sub>2</sub> at sea level and 37 °C), the total ADP  
913 concentration added must be low enough (typically 100 to 300 μM) to allow phosphorylation  
914 to ATP at a coupled O<sub>2</sub> flux that does not lead to O<sub>2</sub> depletion during the transition to State 4.  
915 In contrast, kinetically-saturating ADP concentrations usually are 10-fold higher than 'high  
916 ADP', *e.g.*, 2.5 mM in isolated mitochondria. The abbreviation State 3u is occasionally used in  
917 bioenergetics, to indicate the state of respiration after titration of an uncoupler, without  
918 sufficient emphasis on the fundamental difference between OXPHOS-capacity (*well-coupled*  
919 with an *endogenous* uncoupled component) and ET-capacity (*noncoupled*).

920 **State 4** is a LEAK-state that is obtained only if the mitochondrial preparation is intact  
 921 and well-coupled. Depletion of ADP by phosphorylation to ATP causes a decline of O<sub>2</sub> flux in  
 922 the transition from State 3 to State 4. Under the conditions of State 4, a maximum protonmotive  
 923 force and high ATP/ADP ratio are maintained. The gradual decline of  $Y_{P_{\gg}/O_2}$  towards  
 924 diminishing [ADP] at State 4 must be taken into account for calculation of P<sub>gg</sub>/O<sub>2</sub> ratios (Gnaiger  
 925 2001). State 4 respiration,  $L_T$  (**Table 1**), reflects intrinsic proton leak and ATP hydrolysis  
 926 activity. O<sub>2</sub> flux in State 4 is an overestimation of LEAK-respiration if the contaminating ATP  
 927 hydrolysis activity recycles some ATP to ADP,  $J_{P_{\ll}}$ , which stimulates respiration coupled to  
 928 phosphorylation,  $J_{P_{\gg}} > 0$ . This can be tested by inhibition of the phosphorylation-pathway using  
 929 oligomycin, ensuring that  $J_{P_{\gg}} = 0$  (State 4o). Alternatively, sequential ADP titrations re-  
 930 establish State 3, followed by State 3 to State 4 transitions while sufficient O<sub>2</sub> is available.  
 931 Anoxia may be reached, however, before exhaustion of ADP (State 5).

932 **State 5** is the state after exhaustion of O<sub>2</sub> in a closed respirometric chamber. Diffusion of  
 933 O<sub>2</sub> from the surroundings into the aqueous solution may be a confounding factor preventing  
 934 complete anoxia (Gnaiger 2001). Chance and Williams (1955) provide an alternative definition  
 935 of State 5, which gives it the different meaning of ROX versus anoxia: ‘State 5 may be obtained  
 936 by antimycin A treatment or by anaerobiosis’.

937 In **Table 3**, only States 3 and 4 (and ‘State 2’ in the alternative protocol: addition of fuel  
 938 substrates without ADP; not included in the table) are coupling control states, with the  
 939 restriction that O<sub>2</sub> flux in State 3 may be limited kinetically by non-saturating ADP  
 940 concentrations (**Table 1**).

941

### 942 **3. Normalization: flows and fluxes**

943

#### 944 *3.1. Normalization: system or sample*

945

946 The term *rate* is not sufficiently defined to be useful for reporting data (**Figure 7**). The  
 947 inconsistency of the meanings of rate becomes fully apparent when considering Galileo  
 948 Galilei’s famous principle, that ‘bodies of different weight all fall at the same rate (have a  
 949 constant acceleration)’ (Coopersmith 2010).

950 **Flow per system,  $I$ :** In a generalization of electrical terms, flow as an extensive quantity  
 951 ( $I$ ; per system) is distinguished from flux as a size-specific quantity ( $J$ ; per system size) (**Figure**  
 952 **7A**). Electric current is flow,  $I_{el}$  [ $A \equiv C \cdot s^{-1}$ ] per system (extensive quantity). When dividing this  
 953 extensive quantity by system size (cross-sectional area of a ‘wire’), a size-specific quantity is  
 954 obtained, which is flux (current density),  $J_{el}$  [ $A \cdot m^{-2} = C \cdot s^{-1} \cdot m^{-2}$ ] (**Box 2**).

955

---

### 956 **Box 2: Metabolic flows and fluxes: vectorial and scalar**

957

958 *Flows,  $I_{tr}$* , are defined for all transformations as extensive quantities. Electric charge per  
 959 unit time is electric flow or current,  $I_{el} = dQ_{el} \cdot dt^{-1}$  [ $A$ ]. When expressed per unit cross-sectional  
 960 area,  $A$  [ $m^2$ ], a vector flux is obtained, which is current density (surface-density of flow)  
 961 perpendicular to the direction of flux,  $J_{el} = I_{el} \cdot A^{-1}$  [ $A \cdot m^{-2}$ ] (Cohen et al. 2008). Fluxes with  
 962 *spatial* geometric direction and magnitude are *vectors*. Vector and scalar *fluxes* are related to  
 963 flows as  $J_{tr} = I_{tr} \cdot A^{-1}$  [ $mol \cdot s^{-1} \cdot m^{-2}$ ] and  $J_{tr} = I_{tr} \cdot V^{-1}$  [ $mol \cdot s^{-1} \cdot m^{-3}$ ], expressing flux as an area-specific  
 964 vector or volume-specific vectorial or scalar quantity, respectively (Gnaiger 1993b). We use  
 965 the metre–kilogram–second–ampere (MKSA) international system of units (*SI*) for general  
 966 cases ([m], [kg], [s] and [A]), with decimal *SI* prefixes for specific applications (**Table 4**).

967 We suggest to define: (1) *vectorial* fluxes, which are translocations as functions of  
 968 *gradients* with direction in geometric space in continuous systems; (2) *vectorial* fluxes, which  
 969 describe translocations in discontinuous systems and are restricted to information on  
 970 *compartmental differences* (**Figure 3**, transmembrane proton flux); and (3) *scalar* fluxes, which  
 971 are transformations in a *homogenous* system (**Figure 3**, catabolic O<sub>2</sub> flux,  $J_{KO_2}$ ).

972 Vectorial transmembrane proton fluxes,  $J_{mH^{+}pos}$  and  $J_{mH^{+}neg}$ , are analyzed in a  
 973 heterogenous compartmental system as a quantity with *directional* but not *spatial* information.  
 974 Translocation of protons across the mtIM has a defined direction, either from the negative  
 975 compartment (matrix space; negative, neg–compartment) to the positive compartment (inter-  
 976 membrane space; positive, pos–compartment) or *vice versa* (**Figure 3**). The arrows defining  
 977 the direction of the translocation between the two vesicular compartments may point upwards  
 978 or downwards, right or left, without any implication that these are actual directions in space.  
 979 The pos–compartment is neither above nor below the neg–compartment in a spatial sense, but  
 980 can be visualized arbitrarily in a figure in the upper position (**Figure 3**). In general, the  
 981 *compartmental direction* of vectorial translocation from the neg–compartment to the pos–  
 982 compartment is defined by assigning the initial and final state as *ergodynamic compartments*,  
 983  $H^{+}_{neg} \rightarrow H^{+}_{pos}$  or  $0 = -1 H^{+}_{neg} + 1 H^{+}_{pos}$ , related to work (erg = work) that must be performed to  
 984 lift the proton from a lower to a higher electrochemical potential or from the lower to the higher  
 985 ergodynamic compartment (Gnaiger 1993b).

986 In analogy to *vectorial* translocation, the direction of a *scalar* chemical reaction,  $A \rightarrow B$   
 987 or  $0 = -1 A + 1 B$ , is defined by assigning substrates and products, A and B, as ergodynamic  
 988 compartments.  $O_2$  is defined as a substrate in respiratory  $O_2$  consumption (electron acceptor),  
 989 which together with the fuel substrates (electron donors) comprises the substrate compartment  
 990 of the catabolic reaction. Volume-specific scalar  $O_2$  flux is coupled to vectorial translocation,  
 991 yielding the  $H^{+}_{pos}/O_2$  ratio (**Figure 2B**).

---

992 **Extensive quantities:** An extensive quantity increases proportionally with system size.  
 993 The magnitude of an extensive quantity is completely additive for non-interacting  
 994 subsystems—such as mass or flow expressed per defined system. The magnitude of these  
 995 quantities depends on the extent or size of the system (Cohen *et al.* 2008).

996 **Size-specific quantities:** ‘The adjective *specific* before the name of an extensive quantity  
 997 is often used to mean *divided by mass*’ (Cohen *et al.* 2008). In this system-paradigm, mass-  
 998 specific flux is flow divided by mass of the *system* (the total mass of everything within the  
 999 measuring chamber or reactor). A mass-specific quantity is independent of the extent of non-  
 1000 interacting homogenous subsystems. Tissue-specific quantities (related to the *sample* in  
 1001 contrast to the *system*) are of fundamental interest in the field of comparative mitochondrial  
 1002 physiology, where *specific* refers to the *type of the sample* rather than *mass of the system*. The  
 1003 term *specific*, therefore, must be clarified; *sample-specific*, e.g., muscle mass-specific  
 1004 normalization, is distinguished from *system-specific* quantities (mass or volume; **Figure 7**).

### 1007 3.2. Normalization for system-size: flux per chamber volume

1008 **System-specific flux,  $J_{V,O_2}$ :** The experimental system (experimental chamber) is part of  
 1009 the measurement apparatus, separated from the environment as an isolated, closed, open,  
 1010 isothermal or non-isothermal system (**Table 4**). On another level, we distinguish between (1)  
 1011 the *system* with volume  $V$  and mass  $m$  defined by the system boundaries, and (2) the *sample* or  
 1012 *objects* with volume  $V_X$  and mass  $m_X$  that are enclosed in the experimental chamber (**Figure 7**).  
 1013 Metabolic  $O_2$  flow per object,  $I_{O_2/X}$ , increases as the mass of the object is increased. Sample  
 1014 mass-specific  $O_2$  flux,  $J_{O_2/mX}$  should be independent of the mass of the sample studied in the  
 1015 instrument chamber, but system volume-specific  $O_2$  flux,  $J_{V,O_2}$  (per volume of the instrument  
 1016 chamber), should increase in direct proportion to the mass of the sample in the chamber.  
 1017 Whereas  $J_{V,O_2}$  depends on mass-concentration of the sample in the chamber, it should be  
 1018 independent of the chamber (system) volume at constant sample mass. There are practical  
 1019 limitations to increase the mass-concentration of the sample in the chamber, when one is  
 1020 concerned about crowding effects and instrumental time resolution.

1022 **Figure 7. Flow and flux, and**  
 1023 **normalization in structure-**  
 1024 **function analysis**

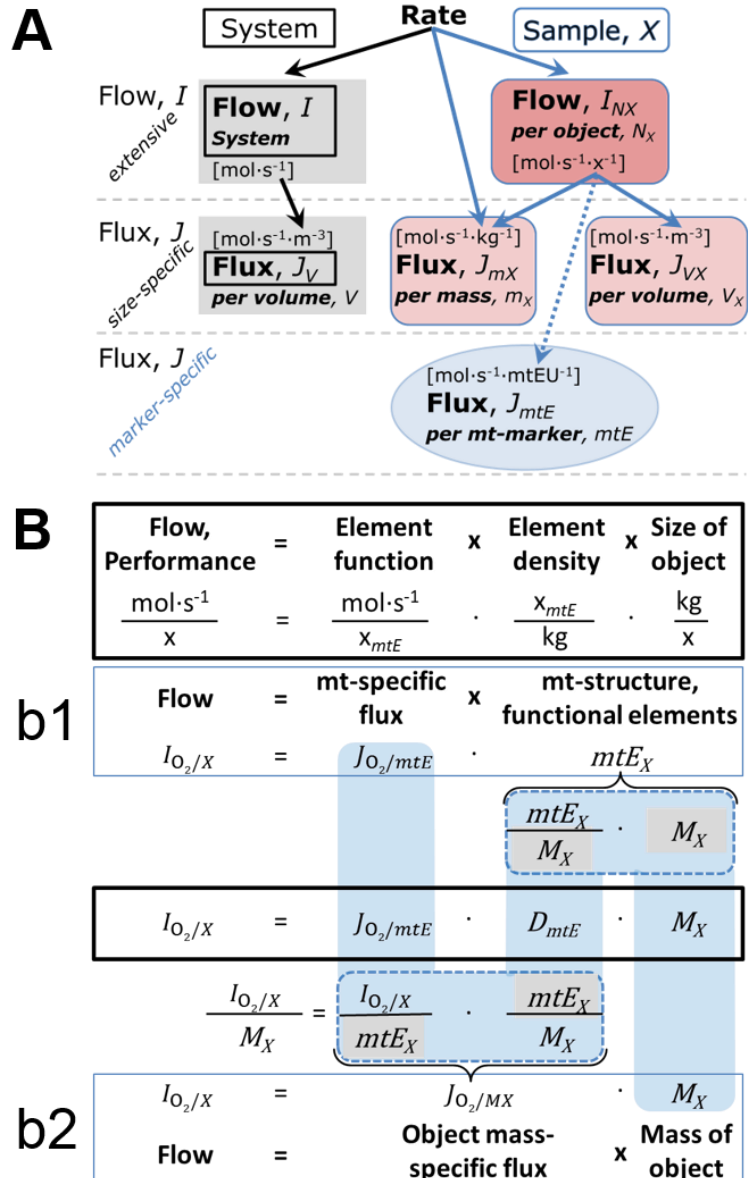
1025 (A) Different meanings of rate  
 1026 may lead to confusion, if the  
 1027 normalization is not sufficiently  
 1028 specified. Results are frequently  
 1029 expressed as mass-specific *flux*,  
 1030  $J_{mX}$ , per mg protein, dry or wet  
 1031 weight (mass). Cell volume,  $V_{\text{cell}}$ ,  
 1032 may be used for normalization  
 1033 (volume-specific flux,  $J_{V\text{cell}}$ ),  
 1034 which must be clearly  
 1035 distinguished from flow per cell,  
 1036  $I_{N\text{cell}}$ , or flux,  $J_V$ , expressed for  
 1037 methodological reasons per  
 1038 volume of the measurement  
 1039 system.

1040 (B)  $O_2$  flow,  $I_{O_2/X}$ , is the product  
 1041 of performance per functional  
 1042 element (element function,  
 1043 mitochondria-specific flux),  
 1044 element density (mitochondrial  
 1045 density,  $D_{\text{mtE}}$ ), and size of entity  $X$   
 1046 (mass,  $M_X$ ). (b1) Structured  
 1047 analysis: performance is the  
 1048 product of mitochondrial *function*  
 1049 (mt-specific flux) and *structure*  
 1050 (functional elements;  $D_{\text{mtE}}$  times  
 1051 mass of  $X$ ). (b2) Unstructured  
 1052 analysis: performance is the  
 1053 product of *entity mass-specific*  
 1054 flux,  $J_{O_2/MX} = I_{O_2/X}/M_X = I_{O_2}/m_X$

1055  $[\text{mol}\cdot\text{s}^{-1}\cdot\text{kg}^{-1}]$  and *size of entity*, expressed as mass of  $X$ ;  $M_X = m_X\cdot N_X^{-1} [\text{kg}\cdot\text{x}^{-1}]$ . Modified from  
 1056 Gnaiger (2014). For further details see **Table 4**.

1057

1058 When the reactor volume does not change during the reaction, which is typical for liquid  
 1059 phase reactions, the volume-specific *flux of a chemical reaction*  $r$  is the time derivative of the  
 1060 advancement of the reaction per unit volume,  $J_{V,rB} = d_{r\zeta_B}/dt\cdot V^{-1} [(\text{mol}\cdot\text{s}^{-1})\cdot\text{L}^{-1}]$ . The *rate of*  
 1061 *concentration change* is  $dc_B/dt [(\text{mol}\cdot\text{L}^{-1})\cdot\text{s}^{-1}]$ , where concentration is  $c_B = n_B/V$ . There is a  
 1062 difference between (1)  $J_{V,rO_2} [\text{mol}\cdot\text{s}^{-1}\cdot\text{L}^{-1}]$  and (2) rate of concentration change  $[\text{mol}\cdot\text{L}^{-1}\cdot\text{s}^{-1}]$ .  
 1063 These merge to a single expression only in closed systems. In open systems, external fluxes  
 1064 (such as  $O_2$  supply) are distinguished from internal transformations (catabolic flux,  $O_2$   
 1065 consumption). In a closed system, external flows of all substances are zero and  $O_2$  consumption  
 1066 (internal flow of catabolic reactions  $k$ ),  $I_{kO_2} [\text{pmol}\cdot\text{s}^{-1}]$ , causes a decline of the amount of  $O_2$   
 1067 in the system,  $n_{O_2} [\text{nmol}]$ . Normalization of these quantities for the volume of the system,  $V [\text{L} \equiv$   
 1068  $\text{dm}^3]$ , yields volume-specific  $O_2$  flux,  $J_{V,kO_2} = I_{kO_2}/V [\text{nmol}\cdot\text{s}^{-1}\cdot\text{L}^{-1}]$ , and  $O_2$  concentration,  $[O_2]$   
 1069 or  $c_{O_2} = n_{O_2}/V [\mu\text{mol}\cdot\text{L}^{-1} = \mu\text{M} = \text{nmol}\cdot\text{mL}^{-1}]$ . Instrumental background  $O_2$  flux is due to external  
 1070 flux into a non-ideal closed respirometer; then total volume-specific flux has to be corrected for  
 1071 instrumental background  $O_2$  flux— $O_2$  diffusion into or out of the instrumental chamber.  $J_{V,kO_2}$   
 1072 is relevant mainly for methodological reasons and should be compared with the accuracy of



1073 instrumental resolution of background-corrected flux, *e.g.*,  $\pm 1 \text{ nmol}\cdot\text{s}^{-1}\cdot\text{L}^{-1}$  (Gnaiger 2001).  
 1074 ‘Metabolic’ or catabolic indicates  $\text{O}_2$  flux,  $J_{\text{kO}_2}$ , corrected for: (1) instrumental background  $\text{O}_2$   
 1075 flux; (2) chemical background  $\text{O}_2$  flux due to autoxidation of chemical components added to  
 1076 the incubation medium; and (3)  $R_{\text{ox}}$  for  $\text{O}_2$ -consuming side reactions unrelated to the catabolic  
 1077 pathway k.

1078

### 1079 3.3. Normalization: per sample

1080

1081 The challenges of measuring mitochondrial respiratory flux are matched by those of  
 1082 normalization. Application of common and defined units is required for direct transfer of  
 1083 reported results into a database. The second [s] is the *SI* unit for the base quantity *time*. It is also  
 1084 the standard time-unit used in solution chemical kinetics. A rate may be considered as the  
 1085 numerator and normalization as the complementary denominator, which are tightly linked in  
 1086 reporting the measurements in a format commensurate with the requirements of a database.  
 1087 Normalization (**Table 4**) is guided by physicochemical principles, methodological  
 1088 considerations, and conceptual strategies (**Figure 7**).

1089 **Sample concentration,  $C_{mX}$ :** Normalization for sample concentration is required to  
 1090 report respiratory data. Considering a tissue or cells as the sample, X, the sample mass is  $m_X$   
 1091 [mg], which is frequently measured as wet or dry weight,  $W_w$  or  $W_d$  [mg], respectively, or as  
 1092 amount of tissue or cell protein,  $m_{\text{Protein}}$ . In the case of permeabilized tissues, cells, and  
 1093 homogenates, the sample concentration,  $C_{mX} = m_X/V$  [ $\text{g}\cdot\text{L}^{-1} = \text{mg}\cdot\text{mL}^{-1}$ ], is the mass of the  
 1094 subsample of tissue that is transferred into the instrument chamber.

1095 **Mass-specific flux,  $J_{\text{O}_2/mX}$ :** Mass-specific flux is obtained by expressing respiration per  
 1096 mass of sample,  $m_X$  [mg]. X is the type of sample—isolated mitochondria, tissue homogenate,  
 1097 permeabilized fibres or cells. Volume-specific flux is divided by mass concentration of X,  $J_{\text{O}_2/mX}$   
 1098  $= J_{V,\text{O}_2}/C_{mX}$ ; or flow per cell is divided by mass per cell,  $J_{\text{O}_2/m\text{cell}} = I_{\text{O}_2/\text{cell}}/M_{\text{cell}}$ . If mass-specific  
 1099  $\text{O}_2$  flux is constant and independent of sample size (expressed as mass), then there is no  
 1100 interaction between the subsystems. A 1.5 mg and a 3.0 mg muscle sample respire at identical  
 1101 mass-specific flux. Mass-specific  $\text{O}_2$  flux, however, may change with the mass of a tissue  
 1102 sample, cells or isolated mitochondria in the measuring chamber, in which the nature of the  
 1103 interaction becomes an issue. Therefore, cell density must be optimized, particularly in  
 1104 experiments carried out in wells, considering the confluency of the cell monolayer or clumps  
 1105 of cells (Salabei *et al.* 2014).

1106 **Number concentration,  $C_{NX}$ :**  $C_{NX}$  is the experimental *number concentration* of sample  
 1107 X. In the case of cells or animals, *e.g.*, nematodes,  $C_{NX} = N_X/V$  [ $\text{x}\cdot\text{L}^{-1}$ ], where  $N_X$  is the number  
 1108 of cells or organisms in the chamber (**Table 4**).

1109 **Flow per object,  $I_{\text{O}_2/X}$ :** A special case of normalization is encountered in respiratory  
 1110 studies with permeabilized (or intact) cells. If respiration is expressed per cell, the  $\text{O}_2$  flow per  
 1111 measurement system is replaced by the  $\text{O}_2$  flow per cell,  $I_{\text{O}_2/\text{cell}}$  (**Table 4**).  $\text{O}_2$  flow can be  
 1112 calculated from volume-specific  $\text{O}_2$  flux,  $J_{V,\text{O}_2}$  [ $\text{nmol}\cdot\text{s}^{-1}\cdot\text{L}^{-1}$ ] (per  $V$  of the measurement chamber  
 1113 [L]), divided by the number concentration of cells,  $C_{N\text{cell}} = N_{\text{cell}}/V$  [ $\text{cell}\cdot\text{L}^{-1}$ ], where  $N_{\text{cell}}$  is the  
 1114 number of cells in the chamber. The total cell count is the sum of viable and dead cells,  $N_{\text{cell}} =$   
 1115  $N_{\text{vce}} + N_{\text{dce}}$  (**Table 5**). The cell viability index,  $\text{CVI} = N_{\text{vce}}/N_{\text{cell}}$ , is the ratio of viable cells ( $N_{\text{vce}}$ ;  
 1116 before experimental permeabilization) per total cell count. After experimental permeabilization,  
 1117 all cells are permeabilized,  $N_{\text{pce}} = N_{\text{cell}}$ . The cell viability index can be used to normalize  
 1118 respiration for the number of cells that have been viable before experimental permeabilization,  
 1119  $I_{\text{O}_2/\text{vce}} = I_{\text{O}_2/\text{cell}}/\text{CVI}$ , considering that mitochondrial respiratory dysfunction in dead cells should  
 1120 be eliminated as a confounding factor.

1121 Cellular  $\text{O}_2$  flow can be compared between cells of identical size. To take into account  
 1122 changes and differences in cell size, normalization is required to obtain cell size-specific or  
 1123 mitochondrial marker-specific  $\text{O}_2$  flux (Renner *et al.* 2003).



**Table 4. Sample concentrations and normalization of flux.**

Expression	Symbol	Definition	Unit	Notes
<b>Sample</b>				
identity of sample	$X$	object: cell, tissue, animal, patient		
number of sample entities $X$	$N_X$	number of objects	x	
mass of sample $X$	$m_X$		kg	1
mass of object $X$	$M_X$	$M_X = m_X \cdot N_X^{-1}$	$\text{kg} \cdot \text{x}^{-1}$	1
<b>Mitochondria</b>				
mitochondria	mt	$X = \text{mt}$		
amount of mt-elements	$mtE$	quantity of mt-marker	mtEU	
<b>Concentrations</b>				
object number concentration	$C_{NX}$	$C_{NX} = N_X \cdot V^{-1}$	$\text{x} \cdot \text{m}^{-3}$	2
sample mass concentration	$C_{mX}$	$C_{mX} = m_X \cdot V^{-1}$	$\text{kg} \cdot \text{m}^{-3}$	
mitochondrial concentration	$C_{mtE}$	$C_{mtE} = mtE \cdot V^{-1}$	$\text{mtEU} \cdot \text{m}^{-3}$	3
specific mitochondrial density	$D_{mtE}$	$D_{mtE} = mtE \cdot m_X^{-1}$	$\text{mtEU} \cdot \text{kg}^{-1}$	4
mitochondrial content, $mtE$ per object $X$	$mtE_X$	$mtE_X = mtE \cdot N_X^{-1}$	$\text{mtEU} \cdot \text{x}^{-1}$	5
<b>O<sub>2</sub> flow and flux</b>				
flow, system	$I_{O_2}$	internal flow	$\text{mol} \cdot \text{s}^{-1}$	6
volume-specific flux	$J_{V,O_2}$	$J_{V,O_2} = I_{O_2} \cdot V^{-1}$	$\text{mol} \cdot \text{s}^{-1} \cdot \text{m}^{-3}$	7
flow per object $X$	$I_{O_2/X}$	$I_{O_2/X} = J_{V,O_2} \cdot C_{NX}^{-1}$	$\text{mol} \cdot \text{s}^{-1} \cdot \text{x}^{-1}$	8
mass-specific flux	$J_{O_2/mX}$	$J_{O_2/mX} = J_{V,O_2} \cdot C_{mX}^{-1}$	$\text{mol} \cdot \text{s}^{-1} \cdot \text{kg}^{-1}$	9
mitochondria-specific flux	$J_{O_2/mtE}$	$J_{O_2/mtE} = J_{V,O_2} \cdot C_{mtE}^{-1}$	$\text{mol} \cdot \text{s}^{-1} \cdot \text{mtEU}^{-1}$	10

- 1126 1 Units are given in the MKSA system (**Box 2**). The *SI* prefix k is used for the *SI* base unit of mass (kg  
1127 = 1,000 g). In praxis, various *SI* prefixes are used for convenience, to make numbers easily readable,  
1128 e.g., 1 mg tissue, cell or mitochondrial mass instead of 0.000001 kg.
- 1129 2 In case sample  $X = \text{cells}$ , the object number concentration is  $C_{N_{\text{cell}}} = N_{\text{cell}} \cdot V^{-1}$ , and volume may be  
1130 expressed in [ $\text{dm}^3 \equiv \text{L}$ ] or [ $\text{cm}^3 = \text{mL}$ ]. See **Table 5** for different object types.
- 1131 3 mt-concentration is an experimental variable, dependent on sample concentration: (1)  $C_{mtE} = mtE \cdot V^{-1}$ ;  
1132 (2)  $C_{mtE} = mtE_X \cdot C_{NX}$ ; (3)  $C_{mtE} = C_{mX} \cdot D_{mtE}$ .
- 1133 4 If the amount of mitochondria,  $mtE$ , is expressed as mitochondrial mass, then  $D_{mtE}$  is the mass  
1134 fraction of mitochondria in the sample. If  $mtE$  is expressed as mitochondrial volume,  $V_{\text{mt}}$ , and the  
1135 mass of sample,  $m_X$ , is replaced by volume of sample,  $V_X$ , then  $D_{mtE}$  is the volume fraction of  
1136 mitochondria in the sample.
- 1137 5  $mtE_X = mtE \cdot N_X^{-1} = C_{mtE} \cdot C_{NX}^{-1}$ .
- 1138 6 O<sub>2</sub> can be replaced by other chemicals B to study different reactions, e.g., ATP, H<sub>2</sub>O<sub>2</sub>, or vesicular  
1139 compartmental translocations, e.g., Ca<sup>2+</sup>.
- 1140 7  $I_{O_2}$  and  $V$  are defined per instrument chamber as a system of constant volume (and constant  
1141 temperature), which may be closed or open.  $I_{O_2}$  is abbreviated for  $I_{r,O_2}$ , i.e., the metabolic or internal  
1142 O<sub>2</sub> flow of the chemical reaction  $r$  in which O<sub>2</sub> is consumed, hence the negative stoichiometric  
1143 number,  $\nu_{O_2} = -1$ .  $I_{r,O_2} = d_r n_{O_2} / dt \cdot \nu_{O_2}^{-1}$ . If  $r$  includes all chemical reactions in which O<sub>2</sub> participates, then  
1144  $d_r n_{O_2} = dn_{O_2} - d_e n_{O_2}$ , where  $dn_{O_2}$  is the change in the amount of O<sub>2</sub> in the instrument chamber and  $d_e n_{O_2}$   
1145 is the amount of O<sub>2</sub> added externally to the system. At steady state, by definition  $dn_{O_2} = 0$ , hence  $d_r n_{O_2}$   
1146  $= -d_e n_{O_2}$ .
- 1147 8  $J_{V,O_2}$  is an experimental variable, expressed per volume of the instrument chamber.
- 1148 9  $I_{O_2/X}$  is a physiological variable, depending on the size of entity  $X$ .
- 1149 10 There are many ways to normalize for a mitochondrial marker, that are used in different experimental  
1150 approaches: (1)  $J_{O_2/mtE} = J_{V,O_2} \cdot C_{mtE}^{-1}$ ; (2)  $J_{O_2/mtE} = J_{V,O_2} \cdot C_{mX}^{-1} \cdot D_{mtE}^{-1} = J_{O_2/mX} \cdot D_{mtE}^{-1}$ ; (3)  $J_{O_2/mtE} =$   
1151  $J_{V,O_2} \cdot C_{NX}^{-1} \cdot mtE_X^{-1} = I_{O_2/X} \cdot mtE_X^{-1}$ ; (4)  $J_{O_2/mtE} = I_{O_2} \cdot mtE^{-1}$ . The mt-elemental unit [mtEU] varies between  
1152 different mt-markers.

1153

**Table 5. Sample types, X, abbreviations, and quantification.**

Identity of sample	X	$N_X$	Mass <sup>a</sup>	Volume	mt-Marker
mitochondrial preparation	mt-prep	[x]	[kg]	[m <sup>3</sup> ]	[mtEU]
isolated mitochondria	imt		$m_{mt}$	$V_{mt}$	$mtE$
tissue homogenate	thom		$m_{thom}$		$mtE_{thom}$
permeabilized tissue	pti		$m_{pti}$		$mtE_{pti}$
permeabilized fibre	pfi		$m_{pfi}$		$mtE_{pfi}$
permeabilized cell	pce	$N_{pce}$	$M_{pce}$	$V_{pce}$	$mtE_{pce}$
cells <sup>b</sup>	cell	$N_{cell}$	$M_{cell}$	$V_{cell}$	$mtE_{cell}$
intact cell, viable cell	vce	$N_{vce}$	$M_{vce}$	$V_{vce}$	
dead cell	dce	$N_{dce}$	$M_{dce}$	$V_{dce}$	
organism	org	$N_{org}$	$M_{org}$	$V_{org}$	

1154

<sup>a</sup> Instead of mass, the wet weight or dry weight is frequently stated,  $W_w$  or  $W_d$ .

1155

$m_X$  is mass of the sample [kg],  $M_X$  is mass of the object [ $kg \cdot x^{-1}$ ].

1156

<sup>b</sup> Total cell count,  $N_{cell} = N_{vce} + N_{dce}$

1157

1158

1159

1160

1161

1162

1163

1164

1165

1166

1167

### 3.4. Normalization for mitochondrial content

1168

1169

1170

1171

1172

1173

1174

1175

1176

1177

Tissues can contain multiple cell populations that may have distinct mitochondrial subtypes. Mitochondria undergo dynamic fission and fusion cycles, and can exist in multiple stages and sizes that may be altered by a range of factors. The isolation of mitochondria (often achieved through differential centrifugation) can therefore yield a subsample of the mitochondrial types present in a tissue, depending on the isolation protocols utilized (*e.g.*, centrifugation speed). This possible bias should be taken into account when planning experiments using isolated mitochondria. Different sizes of mitochondria are enriched at specific centrifugation speeds, which can be used strategically for isolation of mitochondrial subpopulations.

1178

1179

1180

1181

1182

1183

1184

1185

Part of the mitochondrial content of a tissue is lost during preparation of isolated mitochondria. The fraction of isolated mitochondria obtained from a tissue sample is expressed as mitochondrial recovery. At a high mitochondrial recovery the fraction of isolated mitochondria is more representative of the total mitochondrial population than in preparations characterized by low recovery. Determination of the mitochondrial recovery and yield is based on measurement of the concentration of a mitochondrial marker in the stock of isolated mitochondria,  $C_{mtE,stock}$ , and crude tissue homogenate,  $C_{mtE,thom}$ , which simultaneously provides information on the specific mitochondrial density in the sample,  $D_{mtE}$  (Table 4).

1186

1187

1188

1189

1190

Normalization is a problematic subject; it is essential to consider the question of the study. If the study aims at comparing tissue performance—such as the effects of a treatment on a specific tissue, then normalization for tissue mass or protein content is appropriate. However, if the aim is to find differences on mitochondrial function independent of mitochondrial density (Table 4), then normalization to a mitochondrial marker is imperative (Figure 7). One cannot

1191 assume that quantitative changes in various markers—such as mitochondrial proteins—  
 1192 necessarily occur in parallel with one another. It should be established that the marker chosen  
 1193 is not selectively altered by the performed treatment. In conclusion, the normalization must  
 1194 reflect the question under investigation to reach a satisfying answer. On the other hand, the goal  
 1195 of comparing results across projects and institutions requires standardization on normalization  
 1196 for entry into a databank.

1197 **Mitochondrial concentration,  $C_{mtE}$ , and mitochondrial markers:** Mitochondrial  
 1198 organelles comprise a dynamic cellular reticulum in various states of fusion and fission. Hence,  
 1199 the definition of an "amount" of mitochondria is often misconceived: mitochondria cannot be  
 1200 counted reliably as a number of occurring elements. Therefore, quantification of the "amount"  
 1201 of mitochondria depends on the measurement of chosen mitochondrial markers. 'Mitochondria  
 1202 are the structural and functional elemental units of cell respiration' (Gnaiger 2014). The  
 1203 quantity of a mitochondrial marker can reflect the amount of *mitochondrial elements, mtE*,  
 1204 expressed in various mitochondrial elemental units [mtEU] specific for each measured mt-  
 1205 marker (**Table 4**). However, since mitochondrial quality may change in response to stimuli—  
 1206 particularly in mitochondrial dysfunction (Campos *et al.* 2017) and after exercise training (Pesta  
 1207 *et al.* 2011) and during aging (Daum *et al.* 2013)—some markers can vary while others are  
 1208 unchanged: (1) Mitochondrial volume and membrane area are structural markers, whereas  
 1209 mitochondrial protein mass is frequently used as a marker for isolated mitochondria. (2)  
 1210 Molecular and enzymatic mitochondrial markers (amounts or activities) can be selected as  
 1211 matrix markers, *e.g.*, citrate synthase activity, mtDNA; mtIM-markers, *e.g.*, cytochrome *c*  
 1212 oxidase activity, *aa<sub>3</sub>* content, cardiolipin, or mtOM-markers, *e.g.*, the voltage-dependent anion  
 1213 channel (VDAC), TOM20. (3) Extending the measurement of mitochondrial marker enzyme  
 1214 activity to mitochondrial pathway capacity, ET- or OXPHOS-capacity can be considered as an  
 1215 integrative functional mitochondrial marker.

1216 Depending on the type of mitochondrial marker, the mitochondrial elements, *mtE*, are  
 1217 expressed in marker-specific units. Mitochondrial concentration in the measurement chamber  
 1218 and the tissue of origin are quantified as (1) a quantity for normalization in functional analyses,  
 1219  $C_{mtE}$ , and (2) a physiological output that is the result of mitochondrial biogenesis and  
 1220 degradation,  $D_{mtE}$ , respectively (**Table 4**). It is recommended, therefore, to distinguish  
 1221 *experimental mitochondrial concentration*,  $C_{mtE} = mtE/V$  and *physiological mitochondrial*  
 1222 *density*,  $D_{mtE} = mtE/m_X$ . Then mitochondrial density is the amount of mitochondrial elements  
 1223 per mass of tissue, which is a biological variable (**Figure 7**). The experimental variable is  
 1224 mitochondrial density multiplied by sample mass concentration in the measuring chamber,  $C_{mtE}$   
 1225  $= D_{mtE} \cdot C_{mX}$ , or mitochondrial content multiplied by sample number concentration,  $C_{mtE} =$   
 1226  $mtE_X \cdot C_{NX}$  (**Table 4**).

1227 **Mitochondria-specific flux,  $J_{O_2/mtE}$ :** Volume-specific metabolic  $O_2$  flux depends on: (1)  
 1228 the sample concentration in the volume of the instrument chamber,  $C_{mX}$ , or  $C_{NX}$ ; (2) the  
 1229 mitochondrial density in the sample,  $D_{mtE} = mtE/m_X$  or  $mtE_X = mtE/N_X$ ; and (3) the specific  
 1230 mitochondrial activity or performance per elemental mitochondrial unit,  $J_{O_2/mtE} = J_{V,O_2}/C_{mtE}$   
 1231  $[mol \cdot s^{-1} \cdot mtEU^{-1}]$  (**Table 4**). Obviously, the numerical results for  $J_{O_2/mtE}$  vary with the type of  
 1232 mitochondrial marker chosen for measurement of *mtE* and  $C_{mtE} = mtE/V [mtEU \cdot m^{-3}]$ .

1233

### 1234 3.5. Evaluation of mitochondrial markers

1235

1236 Different methods are implicated in the quantification of mitochondrial markers and have  
 1237 different strengths. Some problems are common for all mitochondrial markers, *mtE*: (1)  
 1238 Accuracy of measurement is crucial, since even a highly accurate and reproducible  
 1239 measurement of  $O_2$  flux results in an inaccurate and noisy expression if normalized by a biased  
 1240 and noisy measurement of a mitochondrial marker. This problem is acute in mitochondrial  
 1241 respiration because the denominators used (the mitochondrial markers) are often small moieties

1242 of which accurate and precise determination is difficult. This problem can be avoided when O<sub>2</sub>  
1243 fluxes measured in substrate-uncoupler-inhibitor titration protocols are normalized for flux in  
1244 a defined respiratory reference state, which is used as an *internal* marker and yields flux control  
1245 ratios, *FCRs*. *FCRs* are independent of *externally* measured markers and, therefore, are  
1246 statistically robust, considering the limitations of ratios in general (Jasienski and Bazzaz 1999).  
1247 *FCRs* indicate qualitative changes of mitochondrial respiratory control, with highest  
1248 quantitative resolution, separating the effect of mitochondrial density or concentration on  $J_{O_2/mX}$   
1249 and  $I_{O_2/X}$  from that of function per elemental mitochondrial marker,  $J_{O_2/mtE}$  (Pesta *et al.* 2011;  
1250 Gnaiger 2014). (2) If mitochondrial quality does not change and only the amount of  
1251 mitochondria varies as a determinant of mass-specific flux, any marker is equally qualified in  
1252 principle; then in practice selection of the optimum marker depends only on the accuracy and  
1253 precision of measurement of the mitochondrial marker. (3) If mitochondrial flux control ratios  
1254 change, then there may not be any best mitochondrial marker. In general, measurement of  
1255 multiple mitochondrial markers enables a comparison and evaluation of normalization for a  
1256 variety of mitochondrial markers. Particularly during postnatal development, the activity of  
1257 marker enzymes—such as cytochrome *c* oxidase and citrate synthase—follows different time  
1258 courses (Drahota *et al.* 2004). Evaluation of mitochondrial markers in healthy controls is  
1259 insufficient for providing guidelines for application in the diagnosis of pathological states and  
1260 specific treatments.

1261 In line with the concept of the respiratory control ratio (Chance and Williams 1955a), the  
1262 most readily used normalization is that of flux control ratios and flux control factors (Gnaiger  
1263 2014). Selection of the state of maximum flux in a protocol as the reference state has the  
1264 advantages of: (1) internal normalization; (2) statistically validated linearization of the response  
1265 in the range of 0 to 1; and (3) consideration of maximum flux for integrating a large number of  
1266 elemental steps in the OXPHOS- or ET-pathways. This reduces the risk of selecting a functional  
1267 marker that is specifically altered by the treatment or pathology, yet increases the chance that  
1268 the highly integrative pathway is disproportionately affected, *e.g.*, the OXPHOS- rather than  
1269 ET-pathway in case of an enzymatic defect in the phosphorylation-pathway. In this case,  
1270 additional information can be obtained by reporting flux control ratios based on a reference  
1271 state which indicates stable tissue-mass specific flux.

1272 Stereological determination of mitochondrial content via two-dimensional transmission  
1273 electron microscopy can have limitations due to the dynamics of mitochondrial size (Meinild  
1274 Lundby *et al.* 2017). Accurate determination of three-dimensional volume by two-dimensional  
1275 microscopy can be both time consuming and statistically challenging (Larsen *et al.* 2012).

1276 The validity of using mitochondrial marker enzymes (citrate synthase activity, Complex  
1277 I–IV amount or activity) for normalization of flux is limited in part by the same factors that  
1278 apply to flux control ratios. Strong correlations between various mitochondrial markers and  
1279 citrate synthase activity (Reichmann *et al.* 1985; Boushel *et al.* 2007; Mogensen *et al.* 2007)  
1280 are expected in a specific tissue of healthy persons and in disease states not specifically  
1281 targeting citrate synthase. Citrate synthase activity is acutely modifiable by exercise  
1282 (Tonkonogi *et al.* 1997; Leek *et al.* 2001). Evaluation of mitochondrial markers related to a  
1283 selected age and sex cohort cannot be extrapolated to provide recommendations for  
1284 normalization in respirometric diagnosis of disease, in different states of development and  
1285 ageing, different cell types, tissues, and species. mtDNA normalized to nDNA via qPCR is  
1286 correlated to functional mitochondrial markers including OXPHOS- and ET-capacity in some  
1287 cases (Puntschart *et al.* 1995; Wang *et al.* 1999; Menshikova *et al.* 2006; Boushel *et al.* 2007),  
1288 but lack of such correlations have been reported (Menshikova *et al.* 2005; Schultz and Wiesner  
1289 2000; Pesta *et al.* 2011). Several studies indicate a strong correlation between cardiolipin  
1290 content and increase in mitochondrial function with exercise (Menshikova *et al.* 2005;  
1291 Menshikova *et al.* 2007; Larsen *et al.* 2012; Faber *et al.* 2014), but it has not been evaluated as  
1292 a general mitochondrial biomarker in disease. With no single best mitochondrial marker, a good

1293 strategy is to quantify several different biomarkers to minimize the decorrelating effects caused  
 1294 by diseases, treatments, or other factors. Determination of multiple markers, particularly a  
 1295 matrix marker and a marker from the mtIM, allows tracking changes in mitochondrial quality  
 1296 defined by their ratio.

1297

### 1298 3.6. Conversion: units

1299

1300 Many different units have been used to report the O<sub>2</sub> consumption rate, OCR (**Table 6**).  
 1301 *SI* base units provide the common reference to introduce the theoretical principles (**Figure 7**),  
 1302 and are used with appropriately chosen *SI* prefixes to express numerical data in the most  
 1303 practical format, with an effort towards unification within specific areas of application (**Table**  
 1304 **7**). Reporting data in *SI* units—including the mole [mol], coulomb [C], joule [J], and second  
 1305 [s]—should be encouraged, particularly by journals which propose the use of *SI* units.

1306

1307

1308

1309

1310

**Table 6. Conversion of various units used in respirometry and ergometry.**  $e^-$  is the number of electrons or reducing equivalents.  $z_B$  is the charge number of entity B.

1 Unit		Multiplication factor	<i>SI</i> -unit	Note
ng.atom O·s <sup>-1</sup>	(2 e <sup>-</sup> )	0.5	nmol O <sub>2</sub> ·s <sup>-1</sup>	
ng.atom O·min <sup>-1</sup>	(2 e <sup>-</sup> )	8.33	pmol O <sub>2</sub> ·s <sup>-1</sup>	
natom O·min <sup>-1</sup>	(2 e <sup>-</sup> )	8.33	pmol O <sub>2</sub> ·s <sup>-1</sup>	
nmol O <sub>2</sub> ·min <sup>-1</sup>	(4 e <sup>-</sup> )	16.67	pmol O <sub>2</sub> ·s <sup>-1</sup>	
nmol O <sub>2</sub> ·h <sup>-1</sup>	(4 e <sup>-</sup> )	0.2778	pmol O <sub>2</sub> ·s <sup>-1</sup>	
mL O <sub>2</sub> ·min <sup>-1</sup> at STPD <sup>a</sup>		0.744	μmol O <sub>2</sub> ·s <sup>-1</sup>	1
W = J/s at -470 kJ/mol O <sub>2</sub>		-2.128	μmol O <sub>2</sub> ·s <sup>-1</sup>	
mA = mC·s <sup>-1</sup>	(z <sub>H+</sub> = 1)	10.36	nmol H <sup>+</sup> ·s <sup>-1</sup>	2
mA = mC·s <sup>-1</sup>	(z <sub>O2</sub> = 4)	2.59	nmol O <sub>2</sub> ·s <sup>-1</sup>	2
nmol H <sup>+</sup> ·s <sup>-1</sup>	(z <sub>H+</sub> = 1)	0.09649	mA	3
nmol O <sub>2</sub> ·s <sup>-1</sup>	(z <sub>O2</sub> = 4)	0.38594	mA	3

1311

1312

1313

1314

1315

1316

1317

1318

1319

1 At standard temperature and pressure dry (STPD: 0 °C = 273.15 K and 1 atm = 101.325 kPa = 760 mmHg), the molar volume of an ideal gas,  $V_m$ , and  $V_{m,O_2}$  is 22.414 and 22.392 L·mol<sup>-1</sup>, respectively. Rounded to three decimal places, both values yield the conversion factor of 0.744. For comparison at normal temperature and pressure dry (NTPD: 20 °C),  $V_{m,O_2}$  is 24.038 L·mol<sup>-1</sup>. Note that the *SI* standard pressure is 100 kPa.

2 The multiplication factor is  $10^6/(z_B \cdot F)$ .

3 The multiplication factor is  $z_B \cdot F/10^6$ .

1320

1321

1322

1323

1324

1325

1326

1327

1328

1329

Although volume is expressed as m<sup>3</sup> using the *SI* base unit, the litre [dm<sup>3</sup>] is a conventional unit of volume for concentration and is used for most solution chemical kinetics. If one multiplies  $I_{O_2/cell}$  by  $C_{Ncell}$ , then the result will not only be the amount of O<sub>2</sub> [mol] consumed per time [s<sup>-1</sup>] in one litre [L<sup>-1</sup>], but also the change in O<sub>2</sub> concentration per second (for any volume of an ideally closed system). This is ideal for kinetic modeling as it blends with chemical rate equations where concentrations are typically expressed in mol·L<sup>-1</sup> (Wagner *et al.* 2011). In studies of multinuclear cells—such as differentiated skeletal muscle cells—it is easy to determine the number of nuclei but not the total number of cells. A generalized concept, therefore, is obtained by substituting cells by nuclei as the sample entity. This does not hold, however, for enucleated platelets.

1330 For studies of cells, we recommend that respiration be expressed, as far as possible, as:  
 1331 (1) O<sub>2</sub> flux normalized for a mitochondrial marker, for separation of the effects of mitochondrial  
 1332 quality and content on cell respiration (this includes *FCRs* as a normalization for a functional  
 1333 mitochondrial marker); (2) O<sub>2</sub> flux in units of cell volume or mass, for comparison of respiration  
 1334 of cells with different cell size (Renner *et al.* 2003) and with studies on tissue preparations, and  
 1335 (3) O<sub>2</sub> flow in units of attomole (10<sup>-18</sup> mol) of O<sub>2</sub> consumed in a second by each cell  
 1336 [amol·s<sup>-1</sup>·cell<sup>-1</sup>], numerically equivalent to [pmol·s<sup>-1</sup>·10<sup>-6</sup> cells]. This convention allows  
 1337 information to be easily used when designing experiments in which O<sub>2</sub> flow must be considered.  
 1338 For example, to estimate the volume-specific O<sub>2</sub> flux in an instrument chamber that would be  
 1339 expected at a particular cell number concentration, one simply needs to multiply the flow per  
 1340 cell by the number of cells per volume of interest. This provides the amount of O<sub>2</sub> [mol]  
 1341 consumed per time [s<sup>-1</sup>] per unit volume [L<sup>-1</sup>]. At an O<sub>2</sub> flow of 100 amol·s<sup>-1</sup>·cell<sup>-1</sup> and a cell  
 1342 density of 10<sup>9</sup> cells·L<sup>-1</sup> (10<sup>6</sup> cells·mL<sup>-1</sup>), the volume-specific O<sub>2</sub> flux is 100 nmol·s<sup>-1</sup>·L<sup>-1</sup> (100  
 1343 pmol·s<sup>-1</sup>·mL<sup>-1</sup>).

1344 **Table 7. Conversion of units with preservation of numerical values.**

Name	Frequently used unit	Equivalent unit	Note
volume-specific flux, $J_{V,O_2}$	pmol·s <sup>-1</sup> ·mL <sup>-1</sup>	nmol·s <sup>-1</sup> ·L <sup>-1</sup>	1
	mmol·s <sup>-1</sup> ·L <sup>-1</sup>	mol·s <sup>-1</sup> ·m <sup>-3</sup>	
cell-specific flow, $I_{O_2/cell}$	pmol·s <sup>-1</sup> ·10 <sup>-6</sup> cells	amol·s <sup>-1</sup> ·cell <sup>-1</sup>	2
	pmol·s <sup>-1</sup> ·10 <sup>-9</sup> cells	zmol·s <sup>-1</sup> ·cell <sup>-1</sup>	3
cell number concentration, $C_{Nce}$	10 <sup>6</sup> cells·mL <sup>-1</sup>	10 <sup>9</sup> cells·L <sup>-1</sup>	
mitochondrial protein concentration, $C_{mtE}$	0.1 mg·mL <sup>-1</sup>	0.1 g·L <sup>-1</sup>	
mass-specific flux, $J_{O_2/m}$	pmol·s <sup>-1</sup> ·mg <sup>-1</sup>	nmol·s <sup>-1</sup> ·g <sup>-1</sup>	4
catabolic power, $P_k$	μW·10 <sup>-6</sup> cells	pW·cell <sup>-1</sup>	1
Volume	1,000 L	m <sup>3</sup> (1,000 kg)	
	L	dm <sup>3</sup> (kg)	
	mL	cm <sup>3</sup> (g)	
	μL	mm <sup>3</sup> (mg)	
	fL	μm <sup>3</sup> (pg)	5
amount of substance concentration	M = mol·L <sup>-1</sup>	mol·dm <sup>-3</sup>	

1346  
 1347 1 pmol: picomole = 10<sup>-12</sup> mol                      4 nmol: nanomole = 10<sup>-9</sup> mol  
 1348 2 amol: attomole = 10<sup>-18</sup> mol                      5 fL: femtolitre = 10<sup>-15</sup> L  
 1349 3 zmol: zeptomole = 10<sup>-21</sup> mol

1350  
 1351 ET-capacity in human cell types including HEK 293, primary HUVEC and fibroblasts  
 1352 ranges from 50 to 180 amol·s<sup>-1</sup>·cell<sup>-1</sup>, measured in intact cells in the noncoupled state (see  
 1353 Gnaiger 2014). At 100 amol·s<sup>-1</sup>·cell<sup>-1</sup> corrected for *Rox*, the current across the mt-membranes,  
 1354  $I_{H^+e}$ , approximates 193 pA·cell<sup>-1</sup> or 0.2 nA per cell. See Rich (2003) for an extension of  
 1355 quantitative bioenergetics from the molecular to the human scale, with a transmembrane proton  
 1356 flux equivalent to 520 A in an adult at a catabolic power of -110 W. Modelling approaches  
 1357 illustrate the link between protonmotive force and currents (Willis *et al.* 2016).

1358 We consider isolated mitochondria as powerhouses and proton pumps as molecular  
 1359 machines to relate experimental results to energy metabolism of the intact cell. The cellular  
 1360 P<sub>»</sub>/O<sub>2</sub> based on oxidation of glycogen is increased by the glycolytic (fermentative) substrate-  
 1361 level phosphorylation of 3 P<sub>»</sub>/Glyc or 0.5 mol P<sub>»</sub> for each mol O<sub>2</sub> consumed in the complete  
 1362 oxidation of a mol glycosyl unit (Glyc). Adding 0.5 to the mitochondrial P<sub>»</sub>/O<sub>2</sub> ratio of 5.4  
 1363 yields a bioenergetic cell physiological P<sub>»</sub>/O<sub>2</sub> ratio close to 6. Two NADH equivalents are

1364 formed during glycolysis and transported from the cytosol into the mitochondrial matrix, either  
 1365 by the malate-aspartate shuttle or by the glycerophosphate shuttle (**Figure 2A**) resulting in  
 1366 different theoretical yields of ATP generated by mitochondria, the energetic cost of which  
 1367 potentially must be taken into account. Considering also substrate-level phosphorylation in the  
 1368 TCA cycle, this high  $P_{\gg}/O_2$  ratio not only reflects proton translocation and OXPHOS studied  
 1369 in isolation, but integrates mitochondrial physiology with energy transformation in the living  
 1370 cell (Gnaiger 1993a).

1371  
 1372

#### 1373 **4. Conclusions**

1374

1375 Catabolic cell respiration is the process of exergonic and exothermic energy  
 1376 transformation in which scalar redox reactions are coupled to vectorial ion translocation across  
 1377 a semipermeable membrane, which separates the small volume of a bacterial cell or  
 1378 mitochondrion from the larger volume of its surroundings. The electrochemical exergy can be  
 1379 partially conserved in the phosphorylation of ADP to ATP or in ion pumping, or dissipated in  
 1380 an electrochemical short-circuit. Respiration is thus clearly distinguished from fermentation as  
 1381 the counterpart of cellular core energy metabolism. An  $O_2$  flux balance scheme illustrates the  
 1382 relationships and general definitions (**Figures 1 and 2**).

1383 Experimentally, respiration is separated in mitochondrial preparations from the  
 1384 interactions with the fermentative pathways of the intact cell. OXPHOS analysis (**Figure 3**) is  
 1385 based on the study of mitochondrial preparations complementary to bioenergetic investigations  
 1386 of intact cells and organisms—from model organisms to the human species including healthy  
 1387 and diseased persons (patients). Different mechanisms of respiratory uncoupling have to be  
 1388 distinguished (**Figure 4**). Metabolic fluxes measured in defined coupling and pathway control  
 1389 states (**Figures 5 and 6**) provide insights into the meaning of cellular and organismic  
 1390 respiration.

1391 The optimal choice for expressing mitochondrial and cell respiration as  $O_2$  flow per  
 1392 biological sample, and normalization for specific tissue-markers (volume, mass, protein) and  
 1393 mitochondrial markers (volume, protein, content, mtDNA, activity of marker enzymes,  
 1394 respiratory reference state) is guided by the scientific question under study. Interpretation of  
 1395 the data depends critically on appropriate normalization (**Figure 7**).

1396 MitoEAGLE can serve as a gateway to better diagnose mitochondrial respiratory  
 1397 adaptations and defects linked to genetic variation, age-related health risks, sex-specific  
 1398 mitochondrial performance, lifestyle with its effects on degenerative diseases, and thermal and  
 1399 chemical environment. The present recommendations on coupling control states and rates,  
 1400 linked to the concept of the protonmotive force, are focused on studies with mitochondrial  
 1401 preparations (**Box 3**). These will be extended in a series of reports on pathway control of  
 1402 mitochondrial respiration, respiratory states in intact cells, and harmonization of experimental  
 1403 procedures.

1404  
 1405

---

#### 1406 **Box 3: Recommendations for studies with mitochondrial preparations**

1407

- 1408 • Normalization of respiratory rates should be provided as far as possible:
  - 1409 1. *Biophysical normalization*: on a per cell basis as  $O_2$  flow; this may not be possible  
 1410 when dealing with coenocytic organisms or tissues without cross-walls  
 1411 separating individual cells (e.g., filamentous fungi, muscle fibers)
  - 1412 2. *Cellular normalization*: per g protein; per cell- or tissue-mass as mass-specific  
 1413  $O_2$  flux; per cell volume as cell volume-specific flux
  - 1414 3. *Mitochondrial normalization*: per mitochondrial marker as mt-specific flux.

- 1415 With information on cell size and the use of multiple normalizations, maximum potential  
 1416 information is available (Renner *et al.* 2003; Wagner *et al.* 2011; Gnaiger 2014). Reporting  
 1417 flow in a respiratory chamber [ $\text{nmol}\cdot\text{s}^{-1}$ ] is discouraged, since it restricts the analysis to intra-  
 1418 experimental comparison of relative (qualitative) differences.
- 1419 ● Catabolic mitochondrial respiration is distinguished from residual  $\text{O}_2$  consumption. Fluxes  
 1420 in mitochondrial coupling states should be, as far as possible, corrected for residual  $\text{O}_2$   
 1421 consumption.
  - 1422 ● Different mechanisms of uncoupling should be distinguished by defined terms. The tightness  
 1423 of coupling relates to these uncoupling mechanisms, whereas the coupling stoichiometry  
 1424 varies as a function the substrate type involved in ET-pathways with either three or two  
 1425 redox proton pumps operating in series. Separation of tightness of coupling from the  
 1426 pathway-dependent coupling stoichiometry is possible only when the substrate type  
 1427 undergoing oxidation remains the same for respiration in LEAK-, OXPHOS-, and ET-states.  
 1428 In studies of the tightness of coupling, therefore, simple substrate-inhibitor combinations  
 1429 should be applied to exclude a shift in substrate competition which may occur when  
 1430 providing physiological substrate cocktails.
  - 1431 ● In studies of isolated mitochondria, the mitochondrial recovery and yield should be reported.  
 1432 Experimental criteria for evaluation of purity versus integrity should be considered.  
 1433 Mitochondrial markers—such as citrate synthase activity as an enzymatic matrix marker—  
 1434 provide a link to the tissue of origin on the basis of calculating the mitochondrial recovery,  
 1435 *i.e.*, the fraction of mitochondrial marker obtained from a unit mass of tissue. Total  
 1436 mitochondrial protein is frequently applied as a mitochondrial marker, which is restricted to  
 1437 isolated mitochondria.
  - 1438 ● In studies of permeabilized cells, the viability of the cell culture or cell suspension of origin  
 1439 should be reported. Normalization should be evaluated for total cell count or viable cell  
 1440 count.
  - 1441 ● Terms and symbols are summarized in **Table 8**. Their use will facilitate transdisciplinary  
 1442 communication and support further developments towards a consistent theory of  
 1443 bioenergetics and mitochondrial physiology. Technical terms related to and defined with  
 1444 normal words can be used as index terms in databases, support the creation of ontologies  
 1445 towards semantic information processing (MitoPedia), and help in communicating analytical  
 1446 findings as impactful data-driven stories. *‘Making data available without making it*  
 1447 *understandable may be worse than not making it available at all’* (National Academies of  
 1448 Sciences, Engineering, and Medicine 2018). Success will depend on taking next steps: (1)  
 1449 exhaustive text-mining considering Omics data and functional data; (2) network analysis of  
 1450 Omics data with bioinformatics tools; (3) cross-validation with distinct bioinformatics  
 1451 approaches; (4) correlation with functional data; (5) guidelines for biological validation of  
 1452 network data. This is a call to carefully contribute to FAIR principles (Findable, Accessible,  
 1453 Interoperable, Reusable) for the sharing of scientific data.

---

1455  
 1456  
 1457 **Table 8. Terms, symbols, and units.**

Term	Symbol	Unit	Links and comments
1462 alternative quinol oxidase	AOX		Figure 2B
1463 amount of substance B	$n_B$	[mol]	
1464 ATP yield per $\text{O}_2$	$Y_{P\gg\text{O}_2}$		$P\gg\text{O}_2$ ratio measured in any respiratory 1466 state
1467 catabolic reaction	k		Figure 1 and 3
1468 catabolic respiration	$J_{k\text{O}_2}$	<i>varies</i>	Figure 1 and 3



1469	cell number	$N_{\text{cell}}$	[x]	Table 5; $N_{\text{cell}} = N_{\text{vce}} + N_{\text{dce}}$
1470	cell respiration	$J_{\text{rO}_2}$	<i>varies</i>	Figure 1
1471	cell viability index	<i>CVI</i>		$CVI = N_{\text{vce}}/N_{\text{cell}} = 1 - N_{\text{dce}}/N_{\text{cell}}$
1472	Complexes I to IV	CI to CIV		respiratory ET Complexes; Figure 2B
1473	concentration of substance B	$c_B = n_B \cdot V^{-1}$ ; [B]	[mol·m <sup>-3</sup> ]	Box 2
1474	dead cell number	$N_{\text{dce}}$	[x]	Table 5; non-viable cells, loss of plasma membrane barrier function
1475				
1476	electron transfer system	ETS		Figure 2B, Figure 5; state
1477	flow, for substance B	$I_B$	[mol·s <sup>-1</sup> ]	system-related extensive quantity; Figure 7
1478				
1479	flux, for substance B	$J_B$	<i>varies</i>	size-specific quantity; Figure 7
1480	inorganic phosphate	$P_i$		Figure 3
1481	intact cell number, viable cell number	$N_{\text{vce}}$	[x]	Table 5; viable cells, intact of plasma membrane barrier function
1482				
1483	LEAK	LEAK		Table 1, Figure 5; state
1484	mass of sample X	$m_X$	[kg]	Table 4
1485	mass of entity X	$M_X$	[kg]	mass of object X; Table 4
1486	MITOCARTA			<a href="https://www.broadinstitute.org/scientific-community/science/programs/metabolic-disease-program/publications/mitocarta/mitocarta-in-0">https://www.broadinstitute.org/scientific-community/science/programs/metabolic-disease-program/publications/mitocarta/mitocarta-in-0</a>
1487				
1488				
1489				
1490				
1491	MitoPedia			<a href="http://www.bioblast.at/index.php/MitoPedia">http://www.bioblast.at/index.php/MitoPedia</a>
1492	mitochondria or mitochondrial	mt		Box 1
1493	mitochondrial DNA	mtDNA		Box 1
1494	mitochondrial concentration	$C_{\text{mtE}} = \text{mtE} \cdot V^{-1}$	[mtEU·m <sup>-3</sup> ]	Table 4
1495	mitochondrial content	$\text{mtE}_X = \text{mtE} \cdot N_X^{-1}$	[mtEU·x <sup>-1</sup> ]	Table 4
1496	mitochondrial elemental unit	mtEU	<i>varies</i>	Table 4, specific units for mt-marker
1497	mitochondrial inner membrane	mtIM		Figure 2; MIM is widely used; the first M is replaced by mt; Box 1
1498				
1499	mitochondrial outer membrane	mtOM		Figure 2; MOM is widely used; the first M is replaced by mt; Box 1
1500				
1501	mitochondrial recovery	$Y_{\text{mtE}}$		fraction of <i>mtE</i> recovered in sample from the tissue of origin
1502				
1503	mitochondrial yield	$Y_{\text{mtE}/m}$		$Y_{\text{mtE}/m} = Y_{\text{mtE}} \cdot D_{\text{mtE}}$
1504	negative	neg		Figure 3
1505	number concentration of X	$C_{\text{NX}}$	[x·m <sup>-3</sup> ]	Table 4
1506	number of entities X	$N_X$	[x]	Table 4, Figure 7
1507	number of entity B	$N_B$	[x]	Table 4
1508	oxidative phosphorylation	OXPHOS		Table 1, Figure 5; state
1509	oxygen concentration	$c_{\text{O}_2} = n_{\text{O}_2} \cdot V^{-1}$ ; [O <sub>2</sub> ]	[mol·m <sup>-3</sup> ]	Section 3.2
1510	oxygen flux, in reaction r	$J_{\text{rO}_2}$	<i>varies</i>	Figure 1
1511	permeabilized cell number	$N_{\text{pce}}$	[x]	Table 5; experimental permeabilization of plasma membrane; $N_{\text{pce}} = N_{\text{cell}}$
1512				
1513	phosphorylation of ADP to ATP	P»		Section 2.2
1514	positive	pos		Figure 3
1515	proton in the negative compartment	$H^+_{\text{neg}}$		Figure 3
1516	proton in the positive compartment	$H^+_{\text{pos}}$		Figure 3
1517	rate of electron transfer in ET state	$E$		ET-capacity; Table 1
1518	rate of LEAK respiration	$L$		Table 1
1519	rate of oxidative phosphorylation	$P$		OXPHOS capacity; Table 1
1520	rate of residual oxygen consumption	$R_{\text{ox}}$		Table 1, Figure 1
1521	residual oxygen consumption	ROX		Table 1; state
1522	respiratory supercomplex	SC I <sub>n</sub> III <sub>n</sub> IV <sub>n</sub>		Box 1; supramolecular assemblies composed of variable copy numbers ( <i>n</i> ) of CI, CIII and CIV
1523				
1524				
1525	specific mitochondrial density	$D_{\text{mtE}} = \text{mtE} \cdot m_X^{-1}$	[mtEU·kg <sup>-1</sup> ]	Table 4
1526	volume	$V$	[m <sup>3</sup> ]	Table 7
1527	weight, dry weight	$W_d$	[kg]	used as mass of sample X; Figure 7
1528	weight, wet weight	$W_w$	[kg]	used as mass of sample X; Figure 7
1529				

1530 **Acknowledgements**

1531 We thank M. Beno for management assistance. This publication is based upon work from COST  
1532 Action CA15203 MitoEAGLE, supported by COST (European Cooperation in Science and  
1533 Technology), and K-Regio project MitoFit (E.G.).

1534  
1535 **Competing financial interests:** E.G. is founder and CEO of Oroboros Instruments, Innsbruck,  
1536 Austria.

1537  
1538 **References**

- 1539  
1540 Altmann R (1894) Die Elementarorganismen und ihre Beziehungen zu den Zellen. Zweite vermehrte Auflage.  
1541 Verlag Von Veit & Comp, Leipzig:160 pp.  
1542 Beard DA (2005) A biophysical model of the mitochondrial respiratory system and oxidative phosphorylation.  
1543 PLoS Comput Biol 1(4):e36.  
1544 Benda C (1898) Weitere Mitteilungen über die Mitochondria. Verh Dtsch Physiol Ges:376-83.  
1545 Birkedal R, Laasmaa M, Vendelin M (2014) The location of energetic compartments affects energetic  
1546 communication in cardiomyocytes. Front Physiol 5:376.  
1547 Blier PU, Dufresne F, Burton RS (2001) Natural selection and the evolution of mtDNA-encoded peptides:  
1548 evidence for intergenomic co-adaptation. Trends Genet 17:400-6.  
1549 Blier PU, Guderley HE (1993) Mitochondrial activity in rainbow trout red muscle: the effect of temperature on  
1550 the ADP-dependence of ATP synthesis. J Exp Biol 176:145-58.  
1551 Breton S, Beaupré HD, Stewart DT, Hoeh WR, Blier PU (2007) The unusual system of doubly uniparental  
1552 inheritance of mtDNA: isn't one enough? Trends Genet 23:465-74.  
1553 Brown GC (1992) Control of respiration and ATP synthesis in mammalian mitochondria and cells. Biochem J  
1554 284:1-13.  
1555 Calvo SE, Klauser CR, Mootha VK (2016) MitoCarta2.0: an updated inventory of mammalian mitochondrial  
1556 proteins. Nucleic Acids Research 44:D1251-7.  
1557 Calvo SE, Julien O, Clauser KR, Shen H, Kamer KJ, Wells JA, Mootha VK (2017) Comparative analysis of  
1558 mitochondrial N-termini from mouse, human, and yeast. Mol Cell Proteomics 16:512-23.  
1559 Campos JC, Queliconi BB, Bozi LHM, Bechara LRG, Dourado PMM, Andres AM, Jannig PR, Gomes KMS,  
1560 Zambelli VO, Rocha-Resende C, Guatimosim S, Brum PC, Mochly-Rosen D, Gottlieb RA, Kowaltowski AJ,  
1561 Ferreira JCB (2017) Exercise reestablishes autophagic flux and mitochondrial quality control in heart failure.  
1562 Autophagy 13:1304-317.  
1563 Canton M, Luvisetto S, Schmehl I, Azzone GF (1995) The nature of mitochondrial respiration and  
1564 discrimination between membrane and pump properties. Biochem J 310:477-81.  
1565 Carrico C, Meyer JG, He W, Gibson BW, Verdin E (2018) The mitochondrial acylome emerges: proteomics,  
1566 regulation by Sirtuins, and metabolic and disease implications. Cell Metab 27:497-512.  
1567 Chan DC (2006) Mitochondria: dynamic organelles in disease, aging, and development. Cell 125:1241-52.  
1568 Chance B, Williams GR (1955a) Respiratory enzymes in oxidative phosphorylation. I. Kinetics of oxygen  
1569 utilization. J Biol Chem 217:383-93.  
1570 Chance B, Williams GR (1955b) Respiratory enzymes in oxidative phosphorylation: III. The steady state. J Biol  
1571 Chem 217:409-27.  
1572 Chance B, Williams GR (1955c) Respiratory enzymes in oxidative phosphorylation. IV. The respiratory chain. J  
1573 Biol Chem 217:429-38.  
1574 Chance B, Williams GR (1956) The respiratory chain and oxidative phosphorylation. Adv Enzymol Relat Subj  
1575 Biochem 17:65-134.  
1576 Chowdhury SK, Djordjevic J, Albensi B, Fernyhough P (2015) Simultaneous evaluation of substrate-dependent  
1577 oxygen consumption rates and mitochondrial membrane potential by TMRM and safranin in cortical  
1578 mitochondria. Biosci Rep 36:e00286.  
1579 Cobb LJ, Lee C, Xiao J, Yen K, Wong RG, Nakamura HK, Mehta HH, Gao Q, Ashur C, Huffman DM, Wan J,  
1580 Muzumdar R, Barzilai N, Cohen P (2016) Naturally occurring mitochondrial-derived peptides are age-  
1581 dependent regulators of apoptosis, insulin sensitivity, and inflammatory markers. Aging (Albany NY) 8:796-  
1582 809.  
1583 Cohen ER, Cvitas T, Frey JG, Holmström B, Kuchitsu K, Marquardt R, Mills I, Pavese F, Quack M, Stohner J,  
1584 Strauss HL, Takami M, Thor HL (2008) Quantities, units and symbols in physical chemistry, IUPAC Green  
1585 Book, 3rd Edition, 2nd Printing, IUPAC & RSC Publishing, Cambridge.  
1586 Cooper H, Hedges LV, Valentine JC, eds (2009) The handbook of research synthesis and meta-analysis. Russell  
1587 Sage Foundation.  
1588 Coopersmith J (2010) Energy, the subtle concept. The discovery of Feynman's blocks from Leibnitz to Einstein.  
1589 Oxford University Press:400 pp.

- 1590 Cummins J (1998) Mitochondrial DNA in mammalian reproduction. *Rev Reprod* 3:172-82.
- 1591 Dai Q, Shah AA, Garde RV, Yonish BA, Zhang L, Medvitz NA, Miller SE, Hansen EL, Dunn CN, Price TM
- 1592 (2013) A truncated progesterone receptor (PR-M) localizes to the mitochondrion and controls cellular
- 1593 respiration. *Mol Endocrinol* 27:741-53.
- 1594 Daum B, Walter A, Horst A, Osiewacz HD, Kühlbrandt W (2013) Age-dependent dissociation of ATP synthase
- 1595 dimers and loss of inner-membrane cristae in mitochondria. *Proc Natl Acad Sci U S A* 110:15301-6.
- 1596 Divakaruni AS, Brand MD (2011) The regulation and physiology of mitochondrial proton leak. *Physiology*
- 1597 (Bethesda) 26:192-205.
- 1598 Doerrier C, Garcia-Souza LF, Krumschnabel G, Wohlfarter Y, Mészáros AT, Gnaiger E (2018) High-Resolution
- 1599 FluoRespirometry and OXPHOS protocols for human cells, permeabilized fibres from small biopsies of
- 1600 muscle, and isolated mitochondria. *Methods Mol Biol* 1782 (Palmeira CM, Moreno AJ, eds): Mitochondrial
- 1601 Bioenergetics, 978-1-4939-7830-4.
- 1602 Doskey CM, van 't Erve TJ, Wagner BA, Buettner GR (2015) Moles of a substance per cell is a highly
- 1603 informative dosing metric in cell culture. *PLOS ONE* 10:e0132572.
- 1604 Drahota Z, Milerová M, Stieglarová A, Houstek J, Ostádal B (2004) Developmental changes of cytochrome *c*
- 1605 oxidase and citrate synthase in rat heart homogenate. *Physiol Res* 53:119-22.
- 1606 Duarte FV, Palmeira CM, Rolo AP (2014) The role of microRNAs in mitochondria: small players acting wide.
- 1607 *Genes (Basel)* 5:865-86.
- 1608 Ernster L, Schatz G (1981) Mitochondria: a historical review. *J Cell Biol* 91:227s-55s.
- 1609 Estabrook RW (1967) Mitochondrial respiratory control and the polarographic measurement of ADP:O ratios.
- 1610 *Methods Enzymol* 10:41-7.
- 1611 Faber C, Zhu ZJ, Castellino S, Wagner DS, Brown RH, Peterson RA, Gates L, Barton J, Bickett M, Hagerty L,
- 1612 Kimbrough C, Sola M, Bailey D, Jordan H, Elangbam CS (2014) Cardiolipin profiles as a potential
- 1613 biomarker of mitochondrial health in diet-induced obese mice subjected to exercise, diet-restriction and
- 1614 ephedrine treatment. *J Appl Toxicol* 34:1122-9.
- 1615 Fell D (1997) Understanding the control of metabolism. Portland Press.
- 1616 Garlid KD, Beavis AD, Ratkje SK (1989) On the nature of ion leaks in energy-transducing membranes. *Biochim*
- 1617 *Biophys Acta* 976:109-20.
- 1618 Garlid KD, Semrad C, Zinchenko V. Does redox slip contribute significantly to mitochondrial respiration? In:
- 1619 Schuster S, Rigoulet M, Ouhabi R, Mazat J-P, eds (1993) Modern trends in biothermokinetics. Plenum Press,
- 1620 New York, London:287-93.
- 1621 Gerö D, Szabo C (2016) Glucocorticoids suppress mitochondrial oxidant production via upregulation of
- 1622 uncoupling protein 2 in hyperglycemic endothelial cells. *PLoS One* 11:e0154813.
- 1623 Gnaiger E. Efficiency and power strategies under hypoxia. Is low efficiency at high glycolytic ATP production a
- 1624 paradox? In: Surviving Hypoxia: Mechanisms of Control and Adaptation. Hochachka PW, Lutz PL, Sick T,
- 1625 Rosenthal M, Van den Thillart G, eds (1993a) CRC Press, Boca Raton, Ann Arbor, London, Tokyo:77-109.
- 1626 Gnaiger E (1993b) Nonequilibrium thermodynamics of energy transformations. *Pure Appl Chem* 65:1983-2002.
- 1627 Gnaiger E (2001) Bioenergetics at low oxygen: dependence of respiration and phosphorylation on oxygen and
- 1628 adenosine diphosphate supply. *Respir Physiol* 128:277-97.
- 1629 Gnaiger E (2009) Capacity of oxidative phosphorylation in human skeletal muscle. New perspectives of
- 1630 mitochondrial physiology. *Int J Biochem Cell Biol* 41:1837-45.
- 1631 Gnaiger E (2014) Mitochondrial pathways and respiratory control. An introduction to OXPHOS analysis. 4th ed.
- 1632 *Mitochondr Physiol Network* 19.12. Oroboros MiPNet Publications, Innsbruck:80 pp.
- 1633 Gnaiger E, Méndez G, Hand SC (2000) High phosphorylation efficiency and depression of uncoupled respiration
- 1634 in mitochondria under hypoxia. *Proc Natl Acad Sci USA* 97:11080-5.
- 1635 Greggio C, Jha P, Kulkarni SS, Lagarrigue S, Broskey NT, Boutant M, Wang X, Conde Alonso S, Ofori E,
- 1636 Auwerx J, Cantó C, Amati F (2017) Enhanced respiratory chain supercomplex formation in response to
- 1637 exercise in human skeletal muscle. *Cell Metab* 25:301-11.
- 1638 Hinkle PC (2005) P/O ratios of mitochondrial oxidative phosphorylation. *Biochim Biophys Acta* 1706:1-11.
- 1639 Hofstadter DR (1979) Gödel, Escher, Bach: An eternal golden braid. A metaphorical fugue on minds and
- 1640 machines in the spirit of Lewis Carroll. Harvester Press:499 pp.
- 1641 Illaste A, Laasmaa M, Peterson P, Vendelin M (2012) Analysis of molecular movement reveals latticelike
- 1642 obstructions to diffusion in heart muscle cells. *Biophys J* 102:739-48.
- 1643 Jasienski M, Bazzaz FA (1999) The fallacy of ratios and the testability of models in biology. *Oikos* 84:321-26.
- 1644 Jepihhina N, Beraud N, Sepp M, Birkedal R, Vendelin M (2011) Permeabilized rat cardiomyocyte response
- 1645 demonstrates intracellular origin of diffusion obstacles. *Biophys J* 101:2112-21.
- 1646 Klepinin A, Ounpuu L, Guzun R, Chekulayev V, Timohhina N, Tepp K, Shevchuk I, Schlattner U, Kaambre T
- 1647 (2016) Simple oxygraphic analysis for the presence of adenylate kinase 1 and 2 in normal and tumor cells. *J*
- 1648 *Bioenerg Biomembr* 48:531-48.
- 1649 Klingenberg M (2017) UCP1 - A sophisticated energy valve. *Biochimie* 134:19-27.

- 1650 Koit A, Shevchuk I, Ounpuu L, Klepinin A, Chekulayev V, Timohhina N, Tepp K, Puurand M, Truu L, Heck K,  
 1651 Valvere V, Guzun R, Kaambre T (2017) Mitochondrial respiration in human colorectal and breast cancer  
 1652 clinical material is regulated differently. *Oxid Med Cell Longev* 1372640.
- 1653 Komlódi T, Tretter L (2017) Methylene blue stimulates substrate-level phosphorylation catalysed by succinyl-  
 1654 CoA ligase in the citric acid cycle. *Neuropharmacology* 123:287-98.
- 1655 Lane N (2005) *Power, sex, suicide: mitochondria and the meaning of life*. Oxford University Press:354 pp.
- 1656 Larsen S, Nielsen J, Neigaard Nielsen C, Nielsen LB, Wibrand F, Stride N, Schroder HD, Boushel RC, Helge  
 1657 JW, Dela F, Hey-Mogensen M (2012) Biomarkers of mitochondrial content in skeletal muscle of healthy  
 1658 young human subjects. *J Physiol* 590:3349-60.
- 1659 Lee C, Zeng J, Drew BG, Sallam T, Martin-Montalvo A, Wan J, Kim SJ, Mehta H, Hevener AL, de Cabo R,  
 1660 Cohen P (2015) The mitochondrial-derived peptide MOTS-c promotes metabolic homeostasis and reduces  
 1661 obesity and insulin resistance. *Cell Metab* 21:443-54.
- 1662 Lee SR, Kim HK, Song IS, Youm J, Dizon LA, Jeong SH, Ko TH, Heo HJ, Ko KS, Rhee BD, Kim N, Han J  
 1663 (2013) Glucocorticoids and their receptors: insights into specific roles in mitochondria. *Prog Biophys Mol*  
 1664 *Biol* 112:44-54.
- 1665 Leek BT, Mudaliar SR, Henry R, Mathieu-Costello O, Richardson RS (2001) Effect of acute exercise on citrate  
 1666 synthase activity in untrained and trained human skeletal muscle. *Am J Physiol Regul Integr Comp Physiol*  
 1667 280:R441-7.
- 1668 Lemieux H, Blier PU, Gnaiger E (2017) Remodeling pathway control of mitochondrial respiratory capacity by  
 1669 temperature in mouse heart: electron flow through the Q-junction in permeabilized fibers. *Sci Rep* 7:2840.
- 1670 Lenaz G, Tioli G, Falasca AI, Genova ML (2017) Respiratory supercomplexes in mitochondria. In: *Mechanisms*  
 1671 *of primary energy transduction in biology*. M Wikstrom (ed) Royal Society of Chemistry Publishing, London,  
 1672 UK:296-337.
- 1673 Liu S, Roellig DM, Guo Y, Li N, Frace MA, Tang K, Zhang L, Feng Y, Xiao L (2016) Evolution of mitosome  
 1674 metabolism and invasion-related proteins in *Cryptosporidium*. *BMC Genomics* 17:1006.
- 1675 Margulis L (1970) *Origin of eukaryotic cells*. New Haven: Yale University Press.
- 1676 Meinild Lundby AK, Jacobs RA, Gehrig S, de Leur J, Hauser M, Bonne TC, Flück D, Dandanell S, Kirk N,  
 1677 Kaech A, Ziegler U, Larsen S, Lundby C (2018) Exercise training increases skeletal muscle mitochondrial  
 1678 volume density by enlargement of existing mitochondria and not de novo biogenesis. *Acta Physiol* 222,  
 1679 e12905.
- 1680 Menshikova EV, Ritov VB, Fairfull L, Ferrell RE, Kelley DE, Goodpaster BH (2006) Effects of exercise on  
 1681 mitochondrial content and function in aging human skeletal muscle. *J Gerontol A Biol Sci Med Sci* 61:534-  
 1682 40.
- 1683 Menshikova EV, Ritov VB, Ferrell RE, Azuma K, Goodpaster BH, Kelley DE (2007) Characteristics of skeletal  
 1684 muscle mitochondrial biogenesis induced by moderate-intensity exercise and weight loss in obesity. *J Appl*  
 1685 *Physiol* (1985) 103:21-7.
- 1686 Menshikova EV, Ritov VB, Toledo FG, Ferrell RE, Goodpaster BH, Kelley DE (2005) Effects of weight loss  
 1687 and physical activity on skeletal muscle mitochondrial function in obesity. *Am J Physiol Endocrinol Metab*  
 1688 288:E818-25.
- 1689 Miller GA (1991) *The science of words*. Scientific American Library New York:276 pp.
- 1690 Mitchell P (1961) Coupling of phosphorylation to electron and hydrogen transfer by a chemi-osmotic type of  
 1691 mechanism. *Nature* 191:144-8.
- 1692 Mitchell P (2011) Chemiosmotic coupling in oxidative and photosynthetic phosphorylation. *Biochim Biophys*  
 1693 *Acta Bioenergetics* 1807:1507-38.
- 1694 Mogensen M, Sahlin K, Fernström M, Glintborg D, Vind BF, Beck-Nielsen H, Højlund K (2007) Mitochondrial  
 1695 respiration is decreased in skeletal muscle of patients with type 2 diabetes. *Diabetes* 56:1592-9.
- 1696 Mohr PJ, Phillips WD (2015) Dimensionless units in the SI. *Metrologia* 52:40-7.
- 1697 Moreno M, Giacco A, Di Munno C, Goglia F (2017) Direct and rapid effects of 3,5-diiodo-L-thyronine (T2).  
 1698 *Mol Cell Endocrinol* 7207:30092-8.
- 1699 Morrow RM, Picard M, Derbeneva O, Leipzig J, McManus MJ, Gousspillou G, Barbat-Artigas S, Dos Santos C,  
 1700 Hepple RT, Murdock DG, Wallace DC (2017) Mitochondrial energy deficiency leads to hyperproliferation of  
 1701 skeletal muscle mitochondria and enhanced insulin sensitivity. *Proc Natl Acad Sci U S A* 114:2705-10.
- 1702 Murley A, Nunnari J (2016) The emerging network of mitochondria-organelle contacts. *Mol Cell* 61:648-53.
- 1703 National Academies of Sciences, Engineering, and Medicine (2018) *International coordination for science data*  
 1704 *infrastructure: Proceedings of a workshop—in brief*. Washington, DC: The National Academies Press. doi:  
 1705 <https://doi.org/10.17226/25015>.
- 1706 Palmfeldt J, Bross P (2017) Proteomics of human mitochondria. *Mitochondrion* 33:2-14.
- 1707 Paradies G, Paradies V, De Benedictis V, Ruggiero FM, Petrosillo G (2014) Functional role of cardiolipin in  
 1708 mitochondrial bioenergetics. *Biochim Biophys Acta* 1837:408-17.
- 1709 Pesta D, Gnaiger E (2012) High-Resolution Respirometry. OXPHOS protocols for human cells and  
 1710 permeabilized fibres from small biopsies of human muscle. *Methods Mol Biol* 810:25-58.

- 1711 Pesta D, Hoppel F, Macek C, Messner H, Faulhaber M, Kobel C, Parson W, Burtscher M, Schocke M, Gnaiger  
 1712 E (2011) Similar qualitative and quantitative changes of mitochondrial respiration following strength and  
 1713 endurance training in normoxia and hypoxia in sedentary humans. *Am J Physiol Regul Integr Comp Physiol*  
 1714 301:R1078–87.
- 1715 Price TM, Dai Q (2015) The role of a mitochondrial progesterone receptor (PR-M) in progesterone action.  
 1716 *Semin Reprod Med* 33:185-94.
- 1717 Puchowicz MA, Varnes ME, Cohen BH, Friedman NR, Kerr DS, Hoppel CL (2004) Oxidative phosphorylation  
 1718 analysis: assessing the integrated functional activity of human skeletal muscle mitochondria – case studies.  
 1719 *Mitochondrion* 4:377-85. Puntschart A, Claassen H, Jostarndt K, Hoppeler H, Billeter R (1995) mRNAs of  
 1720 enzymes involved in energy metabolism and mtDNA are increased in endurance-trained athletes. *Am J*  
 1721 *Physiol* 269:C619-25.
- 1722 Quiros PM, Mottis A, Auwerx J (2016) Mitonuclear communication in homeostasis and stress. *Nat Rev Mol*  
 1723 *Cell Biol* 17:213-26.
- 1724 Rackham O, Mercer TR, Filipovska A (2012) The human mitochondrial transcriptome and the RNA-binding  
 1725 proteins that regulate its expression. *WIREs RNA* 3:675–95.
- 1726 Reichmann H, Hoppeler H, Mathieu-Costello O, von Bergen F, Pette D (1985) Biochemical and ultrastructural  
 1727 changes of skeletal muscle mitochondria after chronic electrical stimulation in rabbits. *Pflugers Arch* 404:1-  
 1728 9.
- 1729 Renner K, Amberger A, Konwalinka G, Gnaiger E (2003) Changes of mitochondrial respiration, mitochondrial  
 1730 content and cell size after induction of apoptosis in leukemia cells. *Biochim Biophys Acta* 1642:115-23.
- 1731 Rice DW, Alverson AJ, Richardson AO, Young GJ, Sanchez-Puerta MV, Munzinger J, Barry K, Boore JL,  
 1732 Zhang Y, dePamphilis CW, Knox EB, Palmer JD (2016) Horizontal transfer of entire genomes via  
 1733 mitochondrial fusion in the angiosperm *Amborella*. *Science* 342:1468-73.
- 1734 Rich P (2003) Chemiosmotic coupling: The cost of living. *Nature* 421:583.
- 1735 Rostovtseva TK, Sheldon KL, Hassanzadeh E, Monge C, Saks V, Bezrukov SM, Sackett DL (2008) Tubulin  
 1736 binding blocks mitochondrial voltage-dependent anion channel and regulates respiration. *Proc Natl Acad Sci*  
 1737 *USA* 105:18746-51.
- 1738 Rustin P, Parfait B, Chretien D, Bourgeron T, Djouadi F, Bastin J, Rötig A, Munnich A (1996) Fluxes of  
 1739 nicotinamide adenine dinucleotides through mitochondrial membranes in human cultured cells. *J Biol Chem*  
 1740 271:14785-90.
- 1741 Saks VA, Veksler VI, Kuznetsov AV, Kay L, Sikk P, Tiivel T, Tranqui L, Olivares J, Winkler K, Wiedemann F,  
 1742 Kunz WS (1998) Permeabilised cell and skinned fiber techniques in studies of mitochondrial function in  
 1743 vivo. *Mol Cell Biochem* 184:81-100.
- 1744 Salabei JK, Gibb AA, Hill BG (2014) Comprehensive measurement of respiratory activity in permeabilized cells  
 1745 using extracellular flux analysis. *Nat Protoc* 9:421-38.
- 1746 Sazanov LA (2015) A giant molecular proton pump: structure and mechanism of respiratory complex I. *Nat Rev*  
 1747 *Mol Cell Biol* 16:375-88.
- 1748 Schneider TD (2006) Claude Shannon: biologist. The founder of information theory used biology to formulate  
 1749 the channel capacity. *IEEE Eng Med Biol Mag* 25:30-3.
- 1750 Schönfeld P, Dymkowska D, Wojtczak L (2009) Acyl-CoA-induced generation of reactive oxygen species in  
 1751 mitochondrial preparations is due to the presence of peroxisomes. *Free Radic Biol Med* 47:503-9.
- 1752 Schultz J, Wiesner RJ (2000) Proliferation of mitochondria in chronically stimulated rabbit skeletal muscle--  
 1753 transcription of mitochondrial genes and copy number of mitochondrial DNA. *J Bioenerg Biomembr* 32:627-  
 1754 34.
- 1755 Speijer D (2016) Being right on Q: shaping eukaryotic evolution. *Biochem J* 473:4103-27.
- 1756 Sugiura A, Mattie S, Prudent J, McBride HM (2017) Newly born peroxisomes are a hybrid of mitochondrial and  
 1757 ER-derived pre-peroxisomes. *Nature* 542:251-4.
- 1758 Simson P, Jepihhina N, Laasmaa M, Peterson P, Birkedal R, Vendelin M (2016) Restricted ADP movement in  
 1759 cardiomyocytes: Cytosolic diffusion obstacles are complemented with a small number of open mitochondrial  
 1760 voltage-dependent anion channels. *J Mol Cell Cardiol* 97:197-203.
- 1761 Stucki JW, Ineichen EA (1974) Energy dissipation by calcium recycling and the efficiency of calcium transport  
 1762 in rat-liver mitochondria. *Eur J Biochem* 48:365-75.
- 1763 Tonkonogi M, Harris B, Sahlin K (1997) Increased activity of citrate synthase in human skeletal muscle after a  
 1764 single bout of prolonged exercise. *Acta Physiol Scand* 161:435-6.
- 1765 Torralba D, Baixauli F, Sánchez-Madrid F (2016) Mitochondria know no boundaries: mechanisms and functions  
 1766 of intercellular mitochondrial transfer. *Front Cell Dev Biol* 4:107. eCollection 2016.
- 1767 Vamecq J, Schepers L, Parmentier G, Mannaerts GP (1987) Inhibition of peroxisomal fatty acyl-CoA oxidase by  
 1768 antimycin A. *Biochem J* 248:603-7.
- 1769 Waczulikova I, Habodaszova D, Cagalinec M, Ferko M, Ulicna O, Mateasik A, Sikurova L, Ziegelhöffer A  
 1770 (2007) Mitochondrial membrane fluidity, potential, and calcium transients in the myocardium from acute  
 1771 diabetic rats. *Can J Physiol Pharmacol* 85:372-81.

- 1772 Wagner BA, Venkataraman S, Buettner GR (2011) The rate of oxygen utilization by cells. *Free Radic Biol Med*  
1773 51:700-712.
- 1774 Wang H, Hiatt WR, Barstow TJ, Brass EP (1999) Relationships between muscle mitochondrial DNA content,  
1775 mitochondrial enzyme activity and oxidative capacity in man: alterations with disease. *Eur J Appl Physiol*  
1776 *Occup Physiol* 80:22-7.
- 1777 Watt IN, Montgomery MG, Runswick MJ, Leslie AG, Walker JE (2010) Bioenergetic cost of making an  
1778 adenosine triphosphate molecule in animal mitochondria. *Proc Natl Acad Sci U S A* 107:16823-7.
- 1779 Weibel ER, Hoppeler H (2005) Exercise-induced maximal metabolic rate scales with muscle aerobic capacity. *J*  
1780 *Exp Biol* 208:1635-44.
- 1781 White DJ, Wolff JN, Pierson M, Gemmell NJ (2008) Revealing the hidden complexities of mtDNA inheritance.  
1782 *Mol Ecol* 17:4925-42.
- 1783 Wikström M, Hummer G (2012) Stoichiometry of proton translocation by respiratory complex I and its  
1784 mechanistic implications. *Proc Natl Acad Sci U S A* 109:4431-6.
- 1785 Williams EG, Wu Y, Jha P, Dubuis S, Blattmann P, Argmann CA, Houten SM, Amariuta T, Wolski W,  
1786 Zamboni N, Aebersold R, Auwerx J (2016) Systems proteomics of liver mitochondria function. *Science* 352  
1787 (6291):aad0189
- 1788 Willis WT, Jackman MR, Messer JI, Kuzmiak-Glancy S, Glancy B (2016) A simple hydraulic analog model of  
1789 oxidative phosphorylation. *Med Sci Sports Exerc* 48:990-1000.
- 1790